REMARKS

Favorable reconsideration is respectfully requested in view of the following remarks.

I.   CLAIM STATUS

Claims 3-7 and 10 were pending in this application when last examined and stand rejected.

Claim 4-7 were objected to.

No new matter has been added.

II.   ENABLEMENT REJECTION

On page 5 of the Office Action, claims 3 and 10 were rejected under 35 U.S.C. § 112, first paragraph, for not reasonably providing enablement for the genus of prostaglandin D receptor antagonist. Applicants respectfully traverse this rejection.
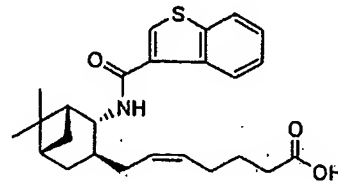
In Examples 6 and 7 in the specification, three prostaglandin D receptor (DP receptor) antagonists, BW A868C, Ramatroban and Pinagladin, all of which are useful for the treatment and prevention of brain injury while having different chemical structures, are described. These three prostaglandin D receptors are shown below:
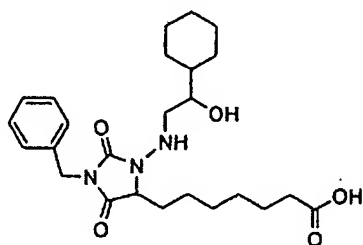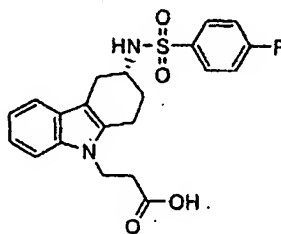
BW A868C   Ramatroban   Pinagladin

In addition to the above-noted three DP receptor antagonists, two additional DP receptor antagonists were evaluated on whether they can treat brain injury.

Specifically, the effect of **TM30089** (3-[(4-fluoro-benzenesulfonyl)-methylamino]-1,2,3,4-tetrahydro-carbazol-9-yl}-acetic acid) (Mathiesen J. et al., Attachment A) or **ONO-4127** Na (-(pbutoxy)benzoyl-2-methylindole-4-acetic acid), (Qu W. et al., Attachment B), which are known to be the antagonist of prostaglandin D receptors was evaluated on a model of stab-

wounded brain injury by a leakage amount of dye to the injured area (Kamimura et al., Nature Medicine, 1998, 4:1078-1080). It was found that the increase in amount of leaked dye noted as a result of brain injury was also suppressed. Enclosed is a Declaration by Dr. Yoshihiro Urade presenting experimental data to support these findings (Attachment C).

It was found that when hereditary or traumatic brain injuries occurs, expression of H-PGDS and DP receptor increase (see Example 3, page 2, lines 24-25, of the specification), and that when an antagonist for DP receptor is administered, the expression of DP receptor decreases (page 3, lines 3-5, of the specification), resulting in reduction of traumatic brain injury (Examples 6 and 7 in the specification).

Thus, it is reasonable to a person of skill in the art that the claimed genus of prostaglandin D receptor antagonist can reduce brain injury caused by prostaglandin D receptor activity without undue experimentation.

Therefore, the specification provides enablement for entire genus of prostaglandin D receptor antagonists.

Applicants further note that the Office asserts that although DP receptor includes both DP-type and CRTH2-type, there is no description of CRTH2-type receptor antagonist. However, Ramatroban (see Example 6 and Fig. 27) and TM 30089 are CRTH2-type receptor antagonists while BW A868C, Pinagladin and ONO-4127 are DP-type receptors. Thus, the antagonist of the present invention can be applied to the entire genus of DP receptor antagonists.

For the above-noted reasons, this rejection is untenable and should be withdrawn.

III. CLAIM OBJECTIONS

On page 11, claims 4-7 are objected to for depending on rejected claims. For the above-noted reasons with regard to claims 3 and 10, this objection is overcome.

IV. OBVIOUSNESS REJECTION

On pages 12-14, claims 3-7 and 10 were rejected under 35 U.S.C. § 103(a) as obvious over Tsuri et al. in view of Wong. Applicants respectfully traverse this rejection.

Tsuri et al. demonstrates that newly synthesized specific DP1-antagonists ameliorated antigen-induced allergic rhinitis (a model of nasal allergy) and antigen-induced allergic asthma (a model of pulmonary allergy) in guinea-pigs. Tsuri et al. summarize at the end of the report

that "this study provides experimental evidence suggesting that the PGD2 receptor antagonists is effective for allergic diseases" (page 3506, left column, lines 11 to 8 from the bottom).

In the study of Tsuri et al., allergic rhinitis was evaluated by measuring intranasal pressure and allergic asthma was evaluated by measuring vascular permeability. These two diseases are induced by the specific antigen, not by brain injury. Although Tsuri et al. demonstrates that DP receptor antagonist is effective for edema of nose and respiratory organs, the edema is allergic edema induced by an allergen.

Wong states that secondary brain injury was triggered by enhancement of vasogenic edema or enhancement vascular permeability. Brain edema is caused by vascular disorder such as trauma and subarachnoid bleeding and not by an allergen. Accordingly, those skilled in the art would not combine Tsuri et al. and Wong to reach the claimed invention. In the claimed invention, DP receptor antagonists were investigated to ameliorate the brain injury, not allergic diseases.

Hurley, et al. and Gilroy, et al. state that inhibition of prostaglandin by cyclooxygenase (COX) inhibitors has shown promise in ameliorating brain injury, but they could not specify the prostaglandins. There are many substances that induce vasogenic edema and enhance vascular permeability. Substances that prevented brain edema and vascular permeability were reported as follows:

1) Sharma H. S., "Neurotrophic factors attenuate microvascular permeability disturbances and axonal injury following trauma to the rat spinalcord", Acta Neurochir. Suppl., 2003, 86:383-8.

2) O'Connor C. A. et al., "Both estrogen and progesterone attenuate edema formation following diffuse traumatic brain injury in rats", Brain Res., 2005, 1062(1-2): 171-4.

3) Moore et al., "Radiation-induced edema is dependent on cyclooxygenase 2 activity in mouse brain", Radiat. Res, 2004, 161(2): 153-60.

4) Bentzer P. et al. "Low-dose prostacyclin improves cortical perfusion following experimental brain injury in the rat", J. Neurotrauma., 2003, 20(5):447-61.

4

5) Patnaik R. et al. "Blockade of histamine H2 receptors attenuate blood-brain barrier permeability, cerebral blood flow disturbances, edema formation and cell reactions following hyperthermic brain injury in the rat", <u>Acta Neurochir. Suppl.</u>, 2000, 76:535-9.

The results of the above-noted articles indicate that it is hard to find that DP receptor antagonists are effective for the brain injury without experimentation. In other words, if a person of skill in the art understood that a compound was effective for treating edema of nose and respiratory organs, such skilled artisan would not understand that such compound can also be used to treat brain injury. In the claimed invention, Applicants actually proofed and ascertained the preventive effects of DP antagonist on brain injury.

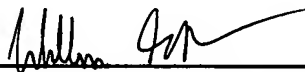For the above-noted reasons, this rejection is untenable and should be withdrawn.

CONCLUSION

In view of the foregoing amendments and remarks, it is respectfully submitted that the present application is in condition for allowance and early notice to that effect is hereby requested.

If the Examiner has any comments or proposals for expediting prosecution, please contact the undersigned attorney at the telephone number below.

Respectfully submitted,

Yoshihiro URADE et al.

By: _____
William R. Schmidt, II
Registration No. 58,327
Attorney for Applicants

WRS/lc
Washington, D.C. 20006-1021
Telephone (202) 721-8200
Facsimile (202) 721-8250
December 16, 2008

ATTACHMENTS

A. Qu, W. et al., "Lipocalin-type prostaglandin D synthase produces prostaglandin D_2 involved in regulation of physiological sleep", PNAS, 2006, 103(47): 17949-17954,

B. Mathiesen, J. et al., "On the Mechanism of Interaction of Potent Surmountable and Insurmountable Antagonists with the Prostaglandin D_2 Receptor CRTH2", Molecular Pharmacology, 2006, 69:2441-1453.

C. Declaration by Dr. Yoshihiro URADE dated December 9, 2008.

Lipocalin-type prostaglandin D synthase produces prostaglandin D$_2$ involved in regulation of physiological sleep

Wei-Min Qu*, Zhi-Li Huang*[†], Xin-Hong Xu*[†], Kosuke Aritake*, Naomi Eguchi*, Fumio Nambu[‡], Shu Narumiya[§], Yoshihiro Urade*, and Osamu Hayaishi*[¶]

*Department of Molecular Behavioral Biology, Osaka Bioscience Institute, Suita, Osaka 565-0874, Japan; [†]State Key Laboratory of Medical Neurobiology, Shanghai Medical College of Fudan University, Shanghai 200032, China; [‡]Ono Pharmaceutical Co., Ltd., Osaka 618-8585, Japan; and [§]Department of Pharmacology, Kyoto University Faculty of Medicine, Kyoto 606-8501, Japan

Prostaglandin (PG) D$_2$ has been proposed to be essential for the initiation and maintenance of the physiological sleep of rats because intracerebroventricular administration of selenium tetrachloride (SeCl$_4$), a selective inhibitor of PGD synthase (PGDS), was shown to reduce promptly and effectively the amounts of sleep during the period of infusion. However, gene knockout (KO) mice of PGDS and prostaglandin D receptor (DP$_1$R) showed essentially the same circadian profiles and daily amounts of sleep as wild-type (WT) mice, raising questions about the involvement of PGD$_2$ in regulating physiological sleep. Here we examined the effect of SeCl$_4$ on the sleep of WT and KO mice for PGDS and DP$_1$R and that of a DP$_1$R antagonist, ONO-4127Na, on the sleep of rats. The i.p. injection of SeCl$_4$ into WT mice decreased the PGD$_2$ content in the brain without affecting the amounts of PGE$_2$ and PGF$_{2\alpha}$. It inhibited sleep dose-dependently and immediately after the administration during the light period when mice normally sleep, increasing the wake time; and the treatment with this compound resulted in a distinct sleep rebound during the following dark period. The SeCl$_4$-induced insomnia was observed in hematopoietic PGDS KO mice but not at all in lipocalin-type PGDS KO, hematopoietic and lipocalin-type PGDS double KO or DP$_1$R KO mice. Furthermore, the DP$_1$R antagonist ONO-4127Na reduced sleep of rats by 30% during infusion into the subarachnoid space under the rostral basal forebrain at 200 pmol/min. These results clearly show that the lipocalin-type PGDS/PGD$_2$/DP$_1$R system plays pivotal roles in the regulation of physiological sleep.

antagonist | enzyme | knockout mice | receptor | selenium tetrachloride

The somnogenic activity of prostaglandin (PG) D$_2$ was originally discovered serendipitously when we microinjected nanomolar quantities of PGD$_2$ in the preoptic area of rats (1). Subsequent studies using a continuous-infusion circadian sleep bioassay system revealed that the effect was specific to PGD$_2$ because other PGs were almost totally inactive (2). Infusion with as little as picomolar quantities per minute was sufficient to induce excess amounts of both non-rapid eye movement (NREM) and rapid eye movement (REM) sleep. Sleep induced by PGD$_2$ was indistinguishable from physiological sleep as judged by several behavioral and electrophysiological criteria, including power spectral analysis (3). PGD$_2$ was not pyrogenic, and it actually caused a slight decrease in the body temperature, as is observed to occur during physiological sleep. These results suggested the possibility that PGD$_2$ might be a sleep hormone (4–7).

PGD$_2$ is the most abundant prostanoid in the brains of rats (8) and other mammals, including humans (9); and it is produced in the brain from the substrate PGH$_2$, a common intermediate of various prostanoids, by the action of PGD synthase (PGDS; PGH$_2$ D-isomerase, EC 5.3.99.2). Two distinct types of PGDS were purified from the brain (10) and spleen (11) of rats in our and other laboratories, and their structures were determined by

x-ray crystallography (12, 13). One was the lipocalin-type PGDS (L-PGDS) (10, 14, 15), mainly expressed in the arachnoid membrane, choroids plexus, and oligodendrocytes in the brain (14, 16); and the other was hematopoietic PGDS (H-PGDS) (17, 18), localized in mast cells (19) and microglia (20, 21). Inorganic tetravalent selenium compounds were found to be potent, relatively specific, and reversible inhibitors of PGDS when tested *in vitro* (22). These inhibitors seemed to interact with the free sulfhydryl group in the active site of PGDS because the inhibition could be reversed by the addition of excess amounts of SH compounds such as glutathione or DTT. In 1991, Matsumura and coworkers (23) administered selenium tetrachloride (SeCl$_4$) into the third ventricle of sleeping rats, and they found that sleep was inhibited almost completely after ≈2 h from the start of the infusion. The effect was reversible because when the infusion was interrupted, sleep was restored. Furthermore, the inhibition was reversed by the simultaneous infusion of SH compounds such as DTT and glutathione, as in the case of the *in vitro* enzyme activity. These results indicated that PGDS plays an essential role in the maintenance of sleep and, therefore, that PGD$_2$ is involved in sleep under physiological conditions in rodents.

Our recent studies with gene knockout (KO) mice for PGDS and prostaglandin D receptors (DP$_1$R) specific for PGD$_2$ showed that mice depleted of these genes did not exhibit NREM sleep rebound after sleep deprivation, suggesting that PGD$_2$ is crucial for the homeostatic regulation of NREM sleep (24). However, KO mice for PGDS or DP$_1$R did not show any changes in the circadian profile and total time of NREM and REM sleep compared with WT mice under baseline conditions, raising questions about the involvement of PGD$_2$ in the regulation of physiological sleep.

In this work, we administered SeCl$_4$ by an i.p. bolus injection during the sleeping period into wild-type (WT) mice as well as into KO mice lacking H-PGDS, L-PGDS, H- and L-PGDS (HL-PGDS), or DP$_1$R, and we studied their sleep–wake behavior. The SeCl$_4$ administration inhibited sleep promptly and effectively in WT and H-PGDS KO mice but not at all in the other three types of KO mice, indicating that SeCl$_4$ inhibited sleep by blocking the endogenous production of PGD$_2$ by

Attachment A

A NREM / REM / Wake

- ONO-4127Na
- Vehicle

Time spent in each stage (min/h)

200 pmol/min

Clock time: 8:00 14:00 20:00 2:00 8:00

B Amount of each stage (min/7 h)

■ ONO-4127Na □ Vehicle

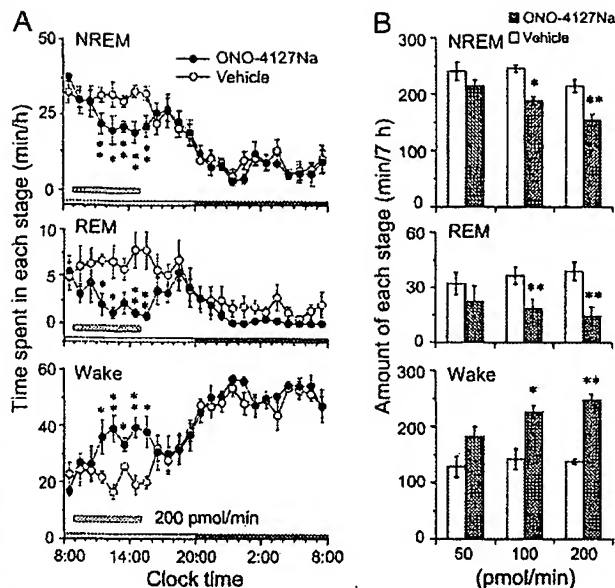NREM / REM / Wake

(pmol/min): 50 100 200

Fig. 1. Sleep-stage distribution produced by ONO-4127Na infusion in rats. (A) Time course changes in ONO-4127Na (200 pmol/min) treatment group. Each circle represents the hourly mean ± SEM of NREM and REM sleep and wakefulness. Open and filled circles indicate the baseline and experimental day profiles, respectively. ONO-4127Na was given between 0900 and 1500 for 6 h, as indicated by the horizontal bar, on the experimental day. The horizontal open and filled bars on the x-axes indicate the 12-h light and 12-h dark periods, respectively. (B) Total time spent in NREM and REM sleep and wakefulness for 7 h; that is, during ONO-4127Na perfusion for 6 h and 1 h postinfusion. Open and filled bars show the profiles for the respective baseline day (vehicle infusion) and experimental day (ONO-4127Na infusion). Values are means ± SEM ($n = 6$). *, $P < 0.05$; **, $P < 0.01$ by the paired t test.

A Enzyme activity (%)

L-PGDS $IC_{50} = 40\ \mu M$

H-PGDS $IC_{50} = 90\ \mu M$

SeCl$_4$ (μM): 10 100 1000

B Contents (pg/brain)

PGD$_2$ $P < 0.01$

PGE$_2$

PGF$_{2\alpha}$

SeCl$_4$ (mg/kg): 0 1.25 2.5 5

Fig. 2. SeCl$_4$ inhibition of the enzymatic activity of both recombinant mouse L-PGDS and H-PGDS in vitro (A) and PGD$_2$, PGE$_2$, and PGF$_{2\alpha}$ contents in the brain 2 h after SeCl$_4$ administration in WT mice (B). Values are means ± SEM ($n = 6$). **, $P < 0.01$ by one-way ANOVA, followed by the Fisher PLSD test.

L-PGDS and not by some nonspecific or general toxic effects of selenium *per se*. We also examined the effect of a DP$_1$R antagonist ONO-4127Na on the sleep of rats, and we found that this antagonist reduced the sleep during infusion into the subarachnoid space under the rostral basal forebrain, in which DP$_1$R is dominantly localized (25). These results indicate again that PGD$_2$ plays a crucial role in the regulation of physiological sleep.

Results

Blockade of DP$_1$R Decreased NREM and REM Sleep in Rats. We infused the DP$_1$R antagonist ONO-4127Na into the subarachnoid space underlying the rostral basal forebrain of rats through a cannula for 6 h from 0900 to 1500 to investigate the changes in the sleep-stage distribution. As shown in Fig. 1A, ONO-4127Na infusion at 200 pmol/min caused a significant decrease in NREM and REM sleep: ONO-4127Na decreased NREM sleep hourly by 30-40%, and it reduced REM sleep by 60-90% commencing ≈2 h after the beginning of ONO-4127Na infusion compared with the baseline. This reduction in sleep time was accompanied by an increase in wakefulness. ONO-4127Na (200 pmol/min) increased the wakefulness time 2.4-fold starting ≈2 h after the beginning of the infusion, and this increase lasted until 1 h after the cessation of infusion. There was no further disruption of the sleep architecture during the subsequent period. Similar time course profiles were observed with a lower concentration of 100 pmol/min. However, ONO-4127Na infusion at 50 pmol/min had little effect on the sleep-stage distribution.

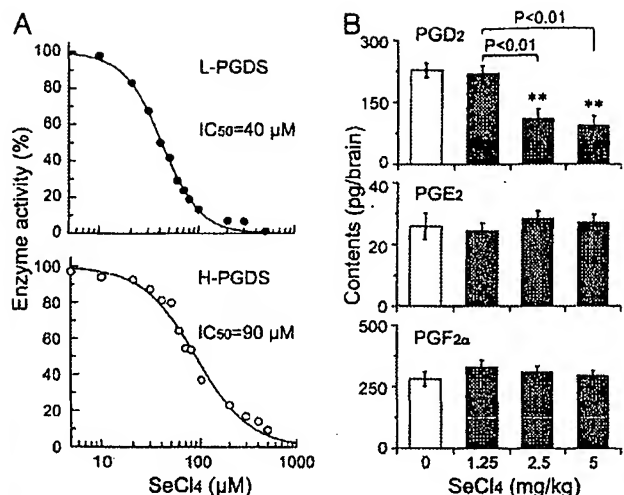We calculated the total time spent in wakefulness and NREM and REM sleep for 7 h, that is, during the ONO-4127Na

perfusion for 6 h and 1 h postinfusion (Fig. 1B). ONO-4127Na given at 100 and 200 pmol/min reduced NREM sleep by 23% and 28% and REM sleep by 49% and 63%, and it increased the total amount of wakefulness by 1.6- and 1.8-fold, respectively, during that 7-h period. There was essentially no difference between ONO-4127Na (50 pmol/min) infusion and the baseline day. These results clearly indicate that ONO-4127Na dose-dependently reduced NREM and REM sleep and concomitantly increased wakefulness.

Inhibition of Mouse Brain PGDS in Vitro and in Vivo by SeCl$_4$. When we examined the effect of SeCl$_4$ on the activities of mouse L-PGDS and H-PGDS in vitro, we found that it inhibited both L-PGDS and H-PGDS efficiently in a concentration-dependent manner, giving IC$_{50}$ values of 40 and 90 μM, respectively (Fig. 2A). To investigate whether SeCl$_4$ inhibits PGDS in vivo, we then determined the PGD$_2$ content in the brain of WT mice at 2 h after an i.p. injection of SeCl$_4$ at a dose of 1.25, 2.5, or 5 mg/kg of body weight. As shown in Fig. 2B, whereas SeCl$_4$ given at 1.25 mg/kg had little effect on the PGD$_2$ content in the brain, at 2.5 and at 5 mg/kg it reduced the PGD$_2$ content by 52% and 59%, respectively, without changing the PGE$_2$ and PGF$_{2\alpha}$ contents, indicating that the SeCl$_4$ administration selectively inhibited the production of PGD$_2$ in the brain in vivo without affecting the production of other PGs.

Inhibition of NREM and REM Sleep of WT Mice by SeCl$_4$ Administration. Next we examined the sleep-wake pattern of WT mice by measuring their electroencephalogram (EEG) and electromyogram (EMG) before and after an i.p. bolus injection of SeCl$_4$ at doses of 1.25, 2.5, 4, and 5 mg/kg at 1100 during the sleep period. The typical time courses of the hourly amounts of NREM and REM sleep and wakefulness and their cumulative amounts for 5 h after injection are summarized in Figs. 3 and 4, respectively. In the case of 1.25 mg/kg SeCl$_4$, the sleep-wake pattern was almost identical before and after the injection, similar to the pattern of PGD$_2$ content in the brain. SeCl$_4$ at 2.5 mg/kg slightly reduced both NREM and REM sleep for 2-3 h after the injection (Fig. 3A). At this dose, the cumulative amounts of NREM and REM sleep for 5 h postinjection significantly decreased by 23% and 44%, respectively, and the amount of
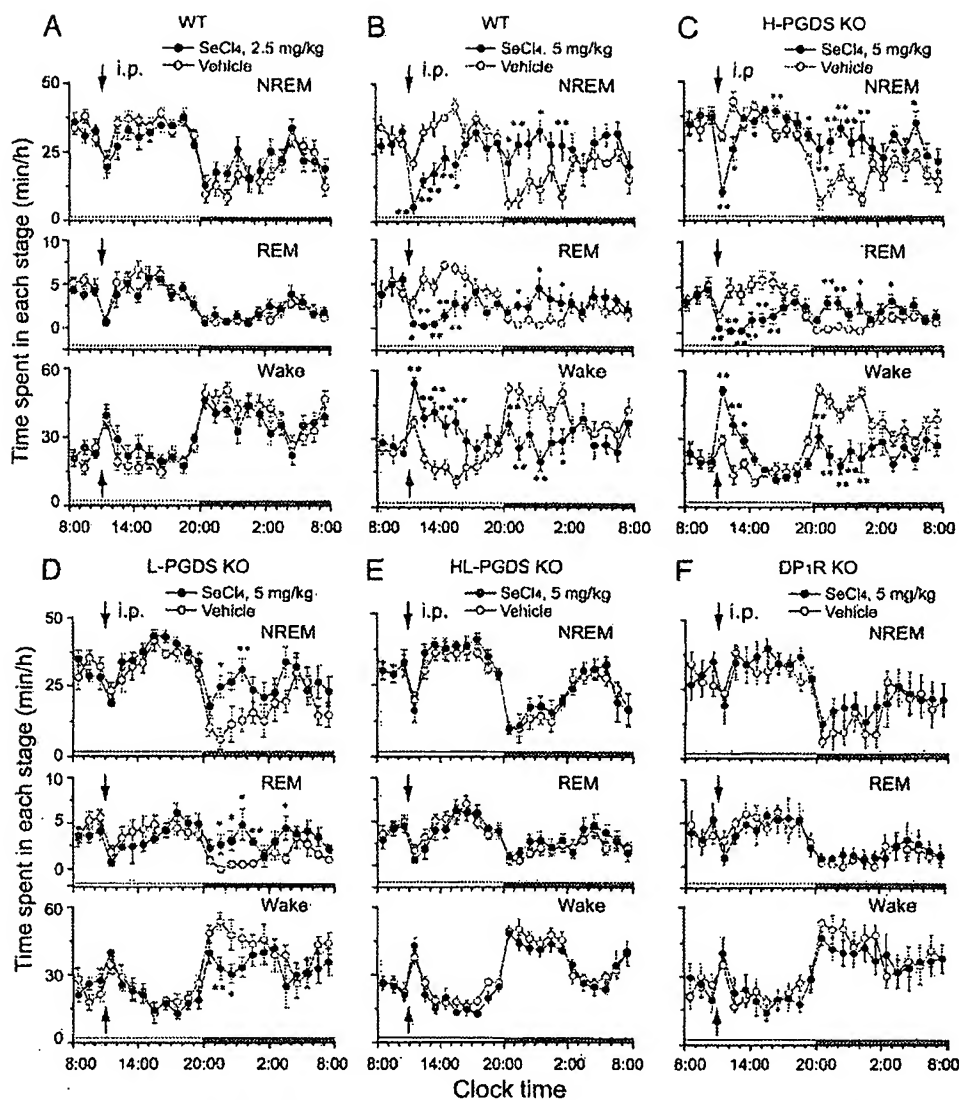
Fig. 3. Time courses of the sleep–wake profiles after i.p. administration of $SeCl_4$ (2.5 and 5 mg/kg) to WT mice (A and B) and $SeCl_4$ (5 mg/kg) to H-PGDS (C), L-PGDS (D), HL-PGDS double (E), and DP_1R (F) KO mice. Each circle represents the hourly mean ± SEM of NREM and REM sleep and wakefulness. Open and filled circles stand for the baseline- and experimental-day profiles, respectively. $SeCl_4$ was given at 1100, as indicated by the arrow, on the experimental day; and the vehicle was used for the baseline day. The horizontal open and filled bars on the x-axes indicate the 12-h light and 12-h dark periods, respectively. Values are means ± SEM (n = 6 or 7). *, $P < 0.05$; **, $P < 0.01$ by the paired t test.

wakefulness increased 1.5-fold (Fig. 4). At doses of 4 and 5 mg/kg $SeCl_4$, both NREM and REM sleep decreased promptly after the injection; and $SeCl_4$-injected mice displayed almost complete insomnia within 1 h. The sleep suppression gradually decreased thereafter, lasting ≈3 and 5 h after the injection of 4 and 5 mg/kg $SeCl_4$, respectively; and both NREM and REM sleep increased remarkably during the following nighttime (Fig. 3B). $SeCl_4$ given at 4 and 5 mg/kg reduced the 5-h cumulative amount of NREM sleep during the daytime by 31% and 45% and that of REM sleep by 63% and 81%, respectively, and it increased that of wakefulness time by 1.7- and 2.1-fold, respectively (Fig. 4). It also induced a strong rebound-like reaction during the following nighttime to increase the 6 h-cumulative amount of NREM sleep 2.2- and 2.4-fold, REM sleep 5.5- and 3.9-fold, and to decrease the amount of wakefulness time by 36% and 41%, respectively. These results revealed that $SeCl_4$ given

during the light period dose dependently inhibited NREM and REM sleep of WT mice and increased both during the following dark period.

Effect of $SeCl_4$ on NREM and REM Sleep of KO Mice Lacking H-PGDS, L-PGDS, HL-PGDS, or DP_1R. We then administered $SeCl_4$ at 5 mg/kg to WT or various KO mice lacking H-PGDS, L-PGDS, HL-PGDS, or DP_1R, and we compared the effect on the sleep–wake cycle between the WT and these KO mice. In H-PGDS KO mice, $SeCl_4$ also inhibited both NREM and REM sleep by 80% and almost completely, respectively, and it increased the wake time ≈2-fold for 1 h after the injection (Fig. 3C). The hourly amounts of NREM sleep and wakefulness returned to the vehicle-injected level within 2–3 h after the administration, but the REM sleep suppression was prolonged for 6 h. H-PGDS KO mice showed strong NREM and REM sleep induction and suppression of
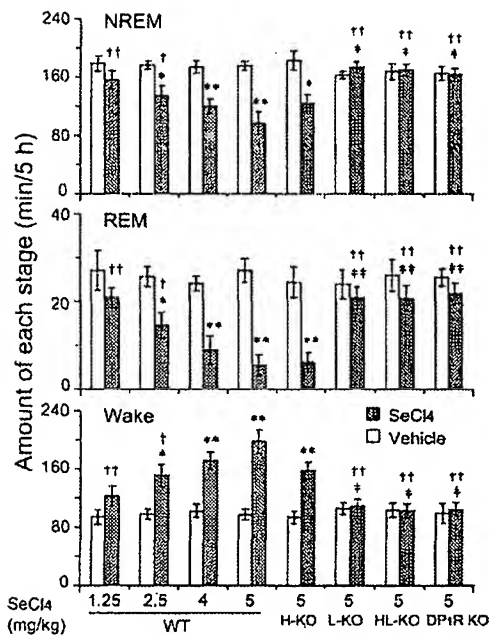
Fig. 4. $SeCl_4$ inhibition of sleep in WT and H-PGDS KO mice, but not in L-PGDS, HL-PGDS double, and DP_1R KO mice. Total time spent in NREM and REM sleep and in wakefulness for 5 h after $SeCl_4$ administration into WT and KO mice is shown. Open and filled bars show the profiles for the baseline and experimental days, when the mice were treated with vehicle and $SeCl_4$, respectively. Values are means ± SEM ($n = 6$ or 7). *, $P < 0.05$; **, $P < 0.01$ compared with its own control; †, $P < 0.05$; ††, $P < 0.01$ compared with WT mice administered $SeCl_4$ at 5 mg/kg; ‡, $P < 0.05$; ‡‡, $P < 0.01$ compared with H-PGDS KO mice i.p. injected with $SeCl_4$ at 5 mg/kg, by two-way ANOVA, followed by the Fisher PLSD test.

wakefulness during the following dark period, similar to the WT mice. In the comparison of the cumulative amounts, NREM and REM sleep for 5 h after the injection decreased by 27% and 78%, respectively, and the wakefulness increased by 1.7-fold (Fig. 4). The cumulative amounts of NREM and REM sleep for 6 h during the following dark period increased 2.4- and 4.1-fold, respectively, and that of wakefulness decreased by 47%. Between the WT and H-PGDS KO mice, there was no statistically significant difference in the responsiveness of NREM and REM sleep and wakefulness to the $SeCl_4$ administration, suggesting that H-PGDS was most likely not involved in the $SeCl_4$-induced insomnia.

In contrast, when L-PGDS KO mice were examined, $SeCl_4$ did not change the amounts of NREM and REM sleep or the time spent in wakefulness at all during the daytime (Figs. 3D and 4), clearly indicating that the sleep inhibition immediately after the administration of $SeCl_4$ depended on L-PGDS. However, interestingly, the $SeCl_4$ administration to L-PGDS KO mice increased both NREM and REM sleep and decreased wakefulness time during the following nighttime (Fig. 3D). The 6-h cumulative amounts of the NREM and REM sleep during the dark period increased almost 2-fold, and that of wakefulness time decreased ≈25%. Between the WT and L-PGDS KO mice, there was no statistically significant difference in the increase in NREM or REM sleep or in the decrease in wakefulness during the nighttime after the $SeCl_4$ administration, indicating that L-PGDS was not involved in the delayed sleep induction by $SeCl_4$. The delayed sleep induction was considered to be mediated by PGD_2 produced by H-PGDS and recognized by DP_1R because it was not observed in HL-PGDS double KO mice or in DP_1R KO mice, as described below.

When $SeCl_4$ was administered to HL-PGDS double KO mice (Fig. 3E) or to DP_1R KO mice (Fig. 3F) under the same experimental conditions, neither the inhibition of sleep immediately after administration of $SeCl_4$ nor the delayed increase in sleep during the night was observed. These results clearly show that $SeCl_4$ was not toxic to inhibit sleep *per se*, but it suppressed sleep by inhibiting the endogenous production of PGD_2, whose information is transferred by DP_1R to induce sleep. These results also suggest that sleep in WT mice is controlled by PGD_2 produced by L-PGDS, rather than H-PGDS, and it is recognized by DP_1R under physiological conditions.

Discussion

The present study showed that $SeCl_4$ inhibited sleep almost immediately after the administration of it to WT mice and H-PGDS KO mice, but it failed to do so in L-PGDS KO, HL-PGDS double KO, and DP_1R KO mice, indicating that L-PGDS is the enzyme responsible for the synthesis of PGD_2 involved in sleep regulation and that the selenium compound inhibited sleep through the L-PGDS/PGD_2/DP_1R system (7).

It is known that selenium compounds are toxic to several species of mammals (26), despite being an essential trace element and the fact that selenocysteine is present in the active site of glutathione peroxidase (27) and a component of other proteins such as selenoprotein P (26). If the observed reduction in sleep had been caused by some toxic effect of selenium, similar changes in the sleep–wake profiles would have been expected in WT, L-, H-PGDS, HL-PGDS double and DP_1R KO mice, let alone the overt behavioral changes that are common consequences of toxicity. Nevertheless, $SeCl_4$ merely caused a significant reduction in the amount of sleep of the WT and H-PGDS KO mice, and it had no effect on the other KO mice, thereby eliminating the possibility of some toxicological effect of $SeCl_4$. In addition, when $SeCl_4$ was infused into the third ventricle of rats during the light period, sleep was inhibited both time- and dose-dependently, and the inhibition was reversed when the infusion was interrupted. Likewise, the effect was reversed by the simultaneous infusion of sulfhydryl compounds such as DTT and reduced glutathione. Furthermore, throughout the sleep-inhibition period caused by selenium administration, all rats displayed normal behaviors similar to those observed during the natural wake phase (23). Recently, Lee *et al.* (28) reported that intracerebroventricular infusion of $SeCl_4$ increased the arousal-like behavior in unanesthetized fetal sheep and that the effect could be abolished by subsequent administration of PGD_2. These findings further indicate that $SeCl_4$-induced sleep inhibition may indeed be attributed to L-PGDS inhibition and not to selenium intoxication.

It is noteworthy that the amount of sleep in L-PGDS KO mice increased during the dark period when $SeCl_4$ was given during the light period, whereas HL-PGDS double KO and DP_1R KO mice were not affected in this way, suggesting that H-PGDS may be involved in the increase in sleep during the dark period. The physiological meaning of this "pseudo-rebound" phenomenon is unknown at present, and further experiments are required to clarify this issue.

Here we showed L-PGDS and DP_1R to be important in sleep induced by PGD_2. When the DP_1R antagonist ONO-4127Na was infused into the subarachnoid space in the rostral basal forebrain of a sleeping rat, where DP_1R are densely localized, sleep was inhibited dose- and time-dependently and reversibly during the period of infusion. However, L-PGDS, DP_1R, and HL-PGDS double KO mice displayed NREM and REM sleep circadian profiles identical to those of WT mice under baseline conditions. Similar phenomena were also found in mice with knockout of other sleep–wake-related genes, such as those for the histamine H_1 receptor (29, 30), orexin (31), and the adenosine A_1 and A_{2A} receptors (32, 33). Considering that sleep is essential for life, it

is not surprising that the sleep-regulatory system would be composed of a complicated network of systems in which the deficiency of one system may be effectively compensated by the other systems during embryonic development (24). However, when mice were subjected to sleep deprivation, L-PGDS KO mice exhibited little NREM sleep rebound, without any increase in PGD$_2$ content in the brain, whereas WT mice displayed a pronounced sleep rebound especially in the NREM sleep, with concomitant increase in PGD$_2$ content in the brain after sleep deprivation (24), indicating that endogenous PGD$_2$ is involved in the homeostatic regulation of NREM sleep.

In conclusion, SeCl$_4$ inhibited sleep in WT mice, concomitant with a reduction in the PGD$_2$ content in the brain. The sleep inhibition was also observed in H-PGDS KO mice, but not in L-PGDS, HL-PGDS double or DP$_1$R KO mice. We conclude that PGD$_2$ is not only involved in the homeostatic regulation of sleep but also essential for the initiation and maintenance of normal circadian sleep under physiological conditions.

Materials and Methods

Animals. L-PGDS KO and H-PGDS KO mice were generated at Osaka Bioscience Institute (Osaka, Japan) and DP$_1$R KO mice, at Kyoto University (Kyoto, Japan), as reported in detail by Eguchi *et al.* (34), Trivedi *et al.* (35), and Matsuoka *et al.* (36), respectively. All of these KO mice were back-crossed to the C57BL/6 strain for >20 generations. Heterozygous mice for either the H- or L-PGDS gene mutation were cross-bred to generate double heterozygous mice. These double heterozygous mice were then cross-bred to produce the WT, H-PGDS KO, L-PGDS KO, and HL-PGDS double KO mice used in this work. Male WT, L-, H-, and HL-PGDS double and DP$_1$R KO mice of the inbred C57BL/6 strain, weighing 25–28 g (11–13 weeks), were maintained at Oriental Bioservice (Kyoto, Japan).

H- and L-PGDS deficiencies were confirmed by Southern blotting and PCR analysis of DNA prepared from clipped tails and by Western blotting with antibodies against H- and L-PGDS proteins, as described in refs. 34 and 35. Physical attributes of the HL-PGDS double KO mice were basically the same as those of the WT, H-PGDS KO, and L-PGDS KO mice as judged by the growth curves of body weight covering up to 40 weeks of age and visual observation of their behaviors.

Male Sprague–Dawley rats weighing 250–320 g (8–10 weeks) were purchased from Shizuoka Laboratory Animal Center (Shizuoka, Japan). Both mice and rats were housed in an insulated sound-proofed recording room maintained at an ambient temperature of 24 ± 0.5°C with a relative humidity of 60 ± 2% on an automatically controlled 12-h light/dark cycle (light on at 0800), and they had free access to food and water. The experimental protocols were approved by the Animal Care Committee of Osaka Bioscience Institute, and every effort was made to minimize the number of animals used as well as any pain and discomfort.

Chemicals. ONO-4127Na was produced and provided by Ono Pharmaceutical Co., Ltd. (Osaka, Japan). This compound exhibited a high specific binding affinity for the DP$_1$R ($K_i = 0.0025$ μM) compared with other prostanoid receptors (Table 1, which is published as supporting information on the PNAS web site) and antagonism toward DP$_1$R (pA$_2$ = 9.73; see Table 2, which is published as supporting information on the PNAS web site), based on the results of competitive binding assays and agonist-stimulated cAMP accumulation assays with mouse DP$_1$R-expressing stable transformants of Chinese hamster ovary cells (37–40). ONO-4127Na is almost insoluble in physiological saline or artificial cerebrospinal fluid, but it is soluble in 5% sucrose with a solubility limit at 5×10^{-4} M. Therefore, the maximum dosage of the drug allowed for infusion into the rat brain was 200 pmol at a rate of 0.4 μl/min. SeCl$_4$ (Wako Pure Chemicals,

Osaka, Japan) was dissolved in sterile saline. Aliquots were prepared and stored frozen at −20°C. For each experiment, the aliquots were thawed, and the pH was adjusted to 7.2 by the addition of 0.2 M NaOH immediately before use.

Enzyme Assay. The effect of SeCl$_4$ on the enzymatic activity of L- and H-PGDS was measured by incubating either enzyme at 25°C for 1 min with [1-^{14}C]PGH$_2$ (final concentration of 40 μM) in 50 μl of 0.1 M Tris·HCl (pH 8.0) containing different concentrations of SeCl$_4$ and 1 mM glutathione (41). [1-^{14}C]PGH$_2$ was prepared from [1-^{14}C]arachidonic acid (2.20 GBq/mmol; PerkinElmer, Wellesley, MA) as described in ref. 10.

PGD$_2$, PGE$_2$, and PGF$_{2\alpha}$ Enzyme Immunoassays. Two hours after SeCl$_4$ had been injected by the i.p. route to WT mice at a dose of 1.25, 2.5, or 5 mg/kg, the brains were harvested and immediately frozen in liquid nitrogen. They were then homogenized in ethanol containing 0.02% HCl at pH 2.0 and centrifuged at $500 \times g$ for 20 min. ^{3}H-labeled PGD$_2$, PGE$_2$, and PGF$_{2\alpha}$ (60 Bq for each per assay; PerkinElmer) were added to the supernatant as tracers for estimation of recovery. The recovery values were ≈60%. PGD$_2$, PGE$_2$, and PGF$_{2\alpha}$ were extracted with ethyl acetate, which was evaporated under nitrogen; and the samples were then separated by a HPLC (Gilson, Middleton, WI) (42). The quantification of PGD$_2$, PGE$_2$, and PGF$_{2\alpha}$ was performed with a PGD$_2$, PGE$_2$, and PGF$_{2\alpha}$ enzyme immunoassay kit for these prostanoids (Cayman Chemicals, Ann Arbor, MI).

Polygraphic Recordings in Rats and Mice. Under pentobarbital anesthesia (50 mg/kg, i.p.), rats underwent surgery for implantation of electrodes for EEG and EMG recordings and placement of a stainless-steel cannula (0.35-mm diameter) for infusion of ONO-4127Na as described earlier (43). The cannulae were inserted in a midline position, 1.1 mm anterior to bregma, to a depth of 7.8–8.0 mm below the dura. The cannulae thus inserted were directed at the subarachnoid space under the rostral basal forebrain, the area defined as a PGD$_2$-sensitive sleep-promoting zone (43). Postoperatively, the rats were housed individually for 8–10 days.

Under pentobarbital anesthesia (50 mg/kg, i.p.), mice were chronically implanted with EEG and EMG electrodes for polysomnographic recordings. The implant consisted of two stainless-steel screws (1-mm diameter) serving as EEG electrodes, inserted, according to the atlas of Franklin and Paxinos (44), through the skull into the cortex (anteroposterior, +1.0 mm and +left-right, −1.5 mm from bregma or lambda); and two insulated, stainless-steel, Teflon-coated wires, serving as EMG electrodes, which were bilaterally placed into both trapezius muscles. All electrodes were attached to a microconnector and fixed to the skull with dental cement (29, 33). Postoperatively, the animals were housed individually for 8–10 days.

The recordings of EEG and EMG were carried out by means of a slip ring, designed so that behavioral movement of the animal would not be restricted. After a 10-day recovery period, the mice or rats were housed individually in transparent barrels and habituated to the recording cable for 3–4 days before starting the polygraphic recordings. The rats were infused continuously with artificial cerebrospinal fluid into the brain at a speed of 0.4 μl/min. Sleep–wakefulness states were monitored for a period of 48 h, which comprised baseline and experimental days. Baseline recordings were taken in each animal for 24 h, beginning at 0800, which served as the control for the same animal. On the next day, ONO-4127Na (50, 100, or 200 pmol/min) was infused into the rat brain between 0900 and 1500 for 6 h. Each mouse was i.p. injected with saline (20 ml/kg of body weight) at 1100 on the 1st day. The next day, again at 1100, SeCl$_4$ was injected i.p. at a dose of 1.25, 2.5, 4, or 5 mg/kg; and EEG/EMG activity was collected for another 24 h.

Cortical EEG and EMG signals were amplified and filtered (EEG, 0.5–30 Hz; EMG, 20–200 Hz), then digitized at a sampling rate of 128 Hz and recorded by using SLEEPSIGN (Kissei Comtec, Nagano, Japan) as described in refs. 29 and 33. The total amounts of wakefulness and NREM and REM sleep were calculated for 7 h after beginning ONO-4127Na infusion and for 5 h after $SeCl_4$ administration. The amounts of the various sleep–wake states were expressed in minutes.

Vigilance State Analysis. Polygraphic recordings were automatically scored offline by 10-s epochs as wakefulness or NREM or REM sleep by SLEEPSIGN according to standard criteria (29). As a final step, defined sleep–wake stages were examined visually, and corrected, if necessary.

Statistical Analysis. All data were expressed as the mean ± SEM ($n = 6$ or 7). For time course data, amounts of the different sleep–wake states were analyzed by the paired t test, with each

animal serving as its own control. For PGD_2, PGE_2, and $PGF_{2\alpha}$ contents in the brain of WT mice and the total amounts of each vigilance stage for 5 h or 7 h after drug treatment, one- or two-way ANOVA followed by the Fisher probable least-squares difference (PLSD) test was used to determine whether the difference among groups and genotypes was statistically significant. In all cases, $P < 0.05$ was taken as the level of significance.

1. Ueno R, Ishikawa Y, Nakayama T, Hayaishi O (1982) *Biochem Biophys Res Commun* 109:576–582.
2. Ueno R, Honda K, Inoue S, Hayaishi O (1983) *Proc Natl Acad Sci USA* 80:1735–1737.
3. Onoe H, Ueno R, Fujita I, Nishino H, Oomura Y, Hayaishi O (1988) *Proc Natl Acad Sci USA* 85:4082–4086.
4. Hayaishi O (1988) *J Biol Chem* 263:14593–14596.
5. Hayaishi O (1991) *FASEB J* 5:2575–2581.
6. Hayaishi O (2002) *J Appl Physiol* 92:863–868.
7. Hayaishi O (2005) *Sleep Circuits and Functions*, ed Luppi P (CRC, Boca Raton), pp 65–82.
8. Narumiya S, Ogorochi T, Nakao K, Hayaishi O (1982) *Life Sci* 31:2093–2103.
9. Ogorochi T, Narumiya S, Mizuno N, Yamashita K, Miyazaki H, Hayaishi O (1984) *J Neurochem* 43:71–82.
10. Urade Y, Fujimoto N, Hayaishi O (1985) *J Biol Chem* 260:12410–12415.
11. Christ-Hazelhof E, Nugteren DH (1979) *Biochim Biophys Acta* 572:43–51.
12. Kanaoka Y, Ago H, Inagaki E, Nanayama T, Miyano M, Kikuno R, Fujii Y, Eguchi N, Toh H, Urade Y, Hayaishi O (1997) *Cell* 90:1085–1095.
13. Irikura D, Kumasaka T, Yamamoto M, Ago H, Miyano M, Kubata KB, Sakai H, Hayaishi O, Urade Y (2003) *J Biochem (Tokyo)* 133:29–32.
14. Urade Y, Kitahama K, Ohishi H, Kaneko T, Mizuno N, Hayaishi O (1993) *Proc Natl Acad Sci USA* 90:9070–9074.
15. Urade Y, Hayaishi O (2000) *Biochim Biophys Acta* 1482:259–271.
16. Beuckmann CT, Lazarus M, Gerashchenko D, Mizoguchi A, Nomura S, Mohri I, Uesugi A, Kaneko T, Mizuno N, Hayaishi O, Urade Y (2000) *J Comp Neurol* 428:62–78.
17. Urade Y, Fujimoto N, Ujihara M, Hayaishi O (1987) *J Biol Chem* 262:3820–3825.
18. Urade Y, Mohri I, Aritake K, Inoue T, Miyano M (2006) *Functional and Structural Biology on the Lipo-network*, eds Morikawa K, Tate S (Transworld Research Network Press, Kerala, India), pp 135–164.
19. Urade Y, Ujihara M, Horiguchi Y, Igarashi M, Nagata A, Ikai K, Hayaishi O (1990) *J Biol Chem* 265:371–375.
20. Mohri I, Eguchi N, Suzuki K, Urade Y, Taniike M (2003) *Glia* 42:263–274.
21. Mohri I, Taniike M, Taniguchi H, Kanekiyo T, Aritake K, Inui T, Fukumoto N, Eguchi N, Kushi A, Sasai H, et al. (2006) *J Neurosci* 26:4383–4393.
22. Islam F, Watanabe Y, Morii H, Hayaishi O (1991) *Arch Biochem Biophys* 289:161–166.
23. Matsumura H, Takahata R, Hayaishi O (1991) *Proc Natl Acad Sci USA* 88:9046–9050.
24. Hayaishi O, Urade Y, Eguchi N, Huang ZL (2004) *Arch Ital Biol* 142:533–539.
25. Mizoguchi A, Eguchi N, Kimura K, Kiyohara Y, Qu WM, Huang ZL, Mochizuki T, Lazarus M, Kobayashi T, Kaneko T, et al. (2001) *Proc Natl Acad Sci USA* 98:11674–11679.
26. Ursini F, Heim S, Kiess M, Maiorino M, Roveri A, Wissing J, Flohe L (1999) *Science* 285:1393–1396.
27. Wingler K, Brigelius-Flohe R (1999) *Biofactors* 10:245–249.
28. Lee B, Hirst JJ, Walker DW (2002) *J Neurosci* 22:5679–5686.
29. Huang ZL, Qu WM, Li WD, Mochizuki T, Eguchi N, Watanabe T, Urade Y, Hayaishi O (2001) *Proc Natl Acad Sci USA* 98:9965–9970.
30. Huang ZL, Mochizuki T, Qu WM, Hong ZY, Watanabe T, Urade Y, Hayaishi O (2006) *Proc Natl Acad Sci USA* 103:4687–4692.
31. Mochizuki T, Crocker A, McCormack S, Yanagisawa M, Sakurai T, Scammell TE (2004) *J Neurosci* 24:6291–6300.
32. Stenberg D, Litonius E, Halldner L, Johansson B, Fredholm BB, Porkka-Heiskanen T (2003) *J Sleep Res* 12:283–290.
33. Huang ZL, Qu WM, Eguchi N, Chen JF, Schwarzschild MA, Fredholm BB, Urade Y, Hayaishi O (2005) *Nat Neurosci* 8:858–859.
34. Eguchi N, Minami T, Shirafuji N, Kanaoka Y, Tanaka T, Nagata A, Yoshida N, Urade Y, Ito S, Hayaishi O (1999) *Proc Natl Acad Sci USA* 96:726–730.
35. Trivedi SG, Newson J, Rajakariar R, Jacques TS, Hannon R, Kanaoka Y, Eguchi N, Colville-Nash P, Gilroy DW (2006) *Proc Natl Acad Sci USA* 103:5179–5184.
36. Matsuoka T, Hirata M, Tanaka H, Takahashi Y, Murata T, Kabashima K, Sugimoto Y, Kobayashi T, Ushikubi F, Aze Y, et al. (2000) *Science* 287:2013–2017.
37. Torisu K, Kobayashi K, Iwahashi M, Egashira H, Nakai Y, Okada Y, Nanbu F, Ohuchida S, Nakai H, Toda M (2004) *Bioorg Med Chem Lett* 14:4557–4562.
38. Torisu K, Kobayashi K, Iwahashi M, Egashira H, Nakai Y, Okada Y, Nanbu F, Ohuchida S, Nakai H, Toda M (2005) *Eur J Med Chem* 40:505–519.
39. Torisu K, Kobayashi K, Iwahashi M, Nakai Y, Onoda T, Nagase T, Sugimoto I, Okada Y, Matsumoto R, Nanbu F, et al. (2004) *Bioorg Med Chem* 12:4685–4700.
40. Torisu K, Kobayashi K, Iwahashi M, Nakai Y, Onoda T, Nagase T, Sugimoto I, Okada Y, Matsumoto R, Nanbu F, et al. (2004) *Bioorg Med Chem Lett* 14:4891–4895.
41. Urade Y, Tanaka T, Eguchi N, Kikuchi M, Kimura H, Toh H, Hayaishi O (1995) *J Biol Chem* 270:1422–1428.
42. Pinzar E, Kanaoka Y, Inui T, Eguchi N, Urade Y, Hayaishi O (2000) *Proc Natl Acad Sci USA* 97:4903–4907.
43. Matsumura H, Nakajima T, Osaka T, Satoh S, Kawase K, Kubo E, Kantha SS, Kasahara K, Hayaishi O (1994) *Proc Natl Acad Sci USA* 91:11998–12002.
44. Franklin KBJ, Paxinos G (1997) *The Mouse Brain in Stereotaxic Coordinates* (Academic, San Diego).

Supporting Tables

Files in this Data Supplement:

Table 1. Binding affinities of ONO-4127Na for various prostanoid receptors

Receptor	mDP_1	mEP_1	mEP_2	mEP 3α	mEP_4	mFP	hEP_2	hIP	hTP
K_i (μM)	0.0025	>8.3	0.013	>4.1	>4.6	>5.8	0.047	0.036	>8.9

Competitive binding experiments for the prostanoid receptors were conducted by using radiolabeled ligands and membrane fractions of Chinese hamster ovary (CHO) cells expressing the prostanoid receptors (see abbreviations defined below): the mouse (m) DP_1 receptor (mDP_1), mEP_1, mEP_2, $mEP_{3\alpha}$, mEP_4, mFP, human (h) EP_2 receptor (hEP_2), hIP, and hTP. Membranes from CHO cells expressing prostanoid receptors were incubated with radiolabeled ligand (2.48 nM [^{3}H] PGD_2 for the mDP_1, 2.48 nM [^{3}H]PGE_2 for the mEP_1, mEP_2 and hEP_2, 14.9 nM [^{3}H]PGE_2 for the $mEP_{3\alpha}$ and mEP_4, 2.48 nM [^{3}H]$PGF_{2\alpha}$ for the mFP, 10 nM [^{3}H]iloprost for the hIP, and 4.95 nM [^{3}H]SQ29548 for the hTP) and various concentrations of ONO-4127Na, natural or synthetic ligands, or vehicle (1% DMSO). Nonspecific binding was achieved by adding excess amounts of unlabeled PGD_2, PGE_2, $PGF_{2\alpha}$, iloprost, or SQ29548, respectively, to the assay buffer. After incubation at room temperature for 20 min for mDP_1 and mEP_1, 30 min for hIP and hTP, or 60 min for mEP_2, hEP_2, $mEP_{3\alpha}$, mEP_4, and mFP, the reaction was terminated by filtration through Whatman GF/B filters. The filters were then washed with ice-cold buffer (1–4), and the radioactivity on the filter was measured with a liquid scintillation counter (TRI-CARB2900TR, Packard). The concentration of the test substance required to inhibit the amounts of the specific binding in the vehicle group by 50% (IC_{50}) was estimated from the regression curve. The K_i value (M) was calculated according to the following equation: $K_i = IC_{50}/(1 + [L]/K_d)$, where [L] and K_d refer to the concentration of radiolabeled ligand and dissociation constant, respectively. Abbreviations: DP_1, PGD_2 receptor; EP_1, EP_2, EP_3, and EP_4, four kinds of PGE_2 receptor subtype; IP, PGI_2 receptor; FP, receptor for $PGF_{2\alpha}$; TP, receptor for thromboxane A_2.

1. Torisu K, Kobayashi K, Iwahashi M, Egashira H, Nakai Y, Okada Y, Nanbu F, Ohuchida S, Nakai H, Toda M (2004) *Bioorg Med Chem Lett* 14:4557–4562.

2. Torisu K, Kobayashi K, Iwahashi M, Egashira H, Nakai Y, Okada Y, Nanbu F, Ohuchida S, Nakai

H, Toda M (2005) *Eur J Med Chem* 40:505–519.

3. Torisu K, Kobayashi K, Iwahashi M, Nakai Y, Onoda T, Nagase T, Sugimoto I, Okada Y, Matsumoto R, Nanbu F, *et al.* (2004) *Bioorg Med Chem* 12:4685–4700.

4. Torisu K, Kobayashi K, Iwahashi M, Nakai Y, Onoda T, Nagase T, Sugimoto I, Okada Y, Matsumoto R, Nanbu F, *et al.* (2004) *Bioorg Med Chem Lett* 14:4891–4895.

Table 2. Antagonism of ONO-4127Na toward agonist-stimulated accumulation of cAMP

	mDP_1	hEP_2	hIP
pA_2 value	9.73	5.81	7.97
	(9.56–9.90)	(5.62–6.00)	(7.76–8.17)
Slope	1.16	1.08	1.04
	(1.07–1.26)	(0.941–1.22)	(0.827–1.25)

( ), 95% confidence intervals

The mDP_1-, hEP_2-, and hIP-CHO cells were stimulated with PGD_2, PGE_2, and iloprost, respectively, in the presence and absence of ONO-4127Na to induce cAMP production. The cAMP content accumulated during 10-min incubation at 37°C was determined by using an RIA cAMP ^{125}I assay system, dual range (Amersham Pharmacia Biotech) according to the manufacturer's instructions. The antagonist action of ONO-4127Na was analyzed by Schild regression analysis, and it is expressed as a pA_2 value, a negative logarithmic concentration required to shift a concentration-response curve of the agonist toward the right by 2-fold. The pA_2 values and slopes are the mean with 95% confidence intervals estimated from five independent experiments.

On the Mechanism of Interaction of Potent Surmountable and Insurmountable Antagonists with the Prostaglandin D2 Receptor CRTH2⑤

Jesper Mosolff Mathiesen, Arthur Christopoulos, Trond Ulven, Julia F. Royer, Mercedes Campillo, Akos Heinemann, Leonardo Pardo, and Evi Kostenis

7TM Pharma A/S, Hørsholm, Denmark (J.M.M., E.K., T.U.); Department of Pharmacology, Monash University, Victoria, Australia (A.C.); Department of Experimental and Clinical Pharmacology, Medical University Graz, Graz, Austria (J.F.R., A.H.); Laboratorio de Medicina Computacional, Unidad de Bioestadistica, Facultad de Medicina, Universidad Autonoma de Barcelona, Barcelona, Spain (M.C., L.P.); and Department of Chemistry, University of Southern Denmark, Odense, Denmark (T.U.)

ABSTRACT

Chemoattractant receptor-homologous molecule expressed on T helper 2 cells (CRTH2) has attracted interest as a potential therapeutic target in inflammatory diseases. Ramatroban, a thromboxane A_2 receptor antagonist with clinical efficacy in allergic rhinitis, was recently found to also display potent CRTH2 antagonistic activity. Here, we present the pharmacological profile of three ramatroban analogs that differ chemically from ramatroban by either a single additional methyl group (TM30642), or an acetic acid instead of a propionic acid side chain (TM30643), or both modifications (TM30089). All three compounds bound to human CRTH2 stably expressed in human embryonic kidney 293 cells with nanomolar affinity. [^{3}H]Prostaglandin D_2 (PGD2) saturation analysis reveals that ramatroban and TM30642 decrease PGD2 affinity, whereas TM30643 and TM30089 exclusively depress ligand binding capacity (B_{max}). Each of the three compounds acted as potent

CRTH2 antagonists, yet the nature of their antagonism differed markedly. In functional assays measuring inhibition of PGD2-mediated 1) guanosine 5'-O-(3-thio)triphosphate binding, 2) β-arrestin translocation, and 3) shape change of human eosinophils endogenously expressing CRTH2, ramatroban, and TM30642 produced surmountable antagonism and parallel rightward shifts of the PGD2 concentration-response curves. For TM30643 and TM30089, this shift was accompanied by a progressive reduction of maximal response. Binding analyses indicated that the functional insurmountability of TM30643 and TM30089 was probably related to long-lasting CRTH2 inhibition mediated via the orthosteric site of the receptor. A mechanistic understanding of insurmountability of CRTH2 antagonists could be fundamental for development of this novel class of anti-inflammatory drugs.

Prostaglandin D_2 (PGD2) is the major prostanoid released by activated mast cells and is implicated as proinflammatory

mediator in diseases such as allergic rhinitis, atopic dermatitis, and asthma (Hata and Breyer, 2004). The prime mode of PGD2 action is through two G protein-coupled receptors referred to as DP/DP1 and CRTH2/DP2, respectively (Boie et al., 1995; Hirai et al., 2001). Both PGD2 receptors transduce extracellular signals predominantly by coupling to heterotrimeric G proteins. DP is positively linked to adenylyl cyclases via $G\alpha_s$ proteins. CRTH2 negatively regulates adenylyl cy-

ABBREVIATIONS: PDG2, prostaglandin D_2; DP, prostaglandin D receptor; CRTH2, chemoattractant receptor-homologous molecule expressed on T helper 2 cells; Th2, T helper 2; TM27868, 1-(4-ethoxyphenyl)-5-methoxy-2-methylindole-3-carboxylic acid; PCR, polymerase chain reaction; ELISA, enzyme-linked immunosorbent assay; β-arr2, β-arrestin2; βarr2-GFP², green fluorescent protein-β-arrestin2-(R393E, R395E) fusion protein; CRTH2-Rluc, Renilla reniformis luciferase-CRTH2 fusion protein; HEK, human embryonic kidney; BRET, bioluminescence resonance energy transfer; HBSS, Hanks' balanced salt solution; DMSO, dimethyl sulfoxide; BSA, bovine serum albumin; PBS, phosphate-buffered saline; GTPγS, guanosine 5'-O-(3-thio)triphosphate; PTX, pertussis toxin; EXP3174, 2-butyl-4-chloro-1-((2'-(1H-tetrazol-5-yl)(1,1'-biphenyl)-4-yl)methyl)-1H-imidazole-5-carboxylic acid; SC-54629, 1-(2,6-dimethylphenyl)-4-butyl-1,3-dihydro-3-((6-(2-(1H-tetrazol-5-yl)phenyl)-3-pyridinyl)methyl)-2H-imidazol-2-one; SC-54628, 1-(2-methylphenyl)-4-butyl-1,3-dihydro-3-((6-(2-(1H-tetrazol-5-yl)phenyl)-3-pyridinyl)methyl)-2H-imidazol-2-one; TM30642, 3-(3-[[(4-fluoro-benzenesulfonyl)-methyl-amino]-1,2,3,4-tetrahydro-carbazol-9-yl]-propionic acid; TM30643, [3-(4-fluoro-benzenesulfonylamino)-1,2,3,4-tetrahydro-carbazol-9-yl]-acetic acid; TM30089, {3-[[(4-fluoro-benzenesulfonyl)-methyl-amino]-1,2,3,4-tetrahydro-carbazol-9-yl]-acetic acid.

clases through $G\alpha_i$ proteins, mobilizes intracellular calcium, and stimulates phosphoinositide 3-kinase, mitogen-activated protein kinases and phospholipase C (Hata and Breyer, 2004). However recent in vitro studies have shown that CRTH2 can also signal via a G protein-independent, arrestin-dependent mechanism that is operative in human eosinophils (Mathiesen et al., 2005). CRTH2 is expressed on Th2 cells, eosinophils, basophils, and monocytes (Nagata et al., 1999; Powell, 2003; Hata and Breyer, 2004), cells that are all established contributors to allergic disease processes. In vitro, CRTH2 activation accounts for PGD2-mediated Th2, eosinophil, and basophil chemotaxis (Hirai et al., 2001; Bohm et al., 2004), up-regulation of surface integrins (Monneret et al., 2003; Powell, 2003), secretion of prototypical Th2 cyto-kines such as interleukin-4, -5, and -13 and proinflammatory chemokines (Tanaka et al., 2004), and increased proliferative responses to T-cell receptor activation (Soler et al., 2005). In vivo, CRTH2 mediates eosinophil mobilization from the bone marrow (Heinemann et al., 2003) and their trafficking into the airways (Shiraishi et al., 2005). The genes encoding CRTH2 and DP have been disrupted individually and in combination by gene targeting (Gonzalo et al., 2005). That study revealed that CRTH2 but not DP is the predominant PGD2 receptor involved in airway inflammation, mucus production, and airway hyper-responsiveness. Although a wealth of evidence suggests a significant proinflammatory role for CRTH2, its precise role in allergic diseases is not fully understood, in part because of the lack of appropriate inhibitors suitable for evaluation of the in vivo relevance of the PGD2-CRTH2 relationship. The orally available small molecule ramatroban (Fig. 1), which was originally developed as a thromboxane A_2 receptor antagonist and is currently marketed in Japan for treatment of allergic rhinitis, has recently been shown to also antagonize CRTH2 with a potency sufficient to account at least in part for the beneficial clinical effects of ramatroban (Sugimoto et al., 2003; Robarge et al., 2005; Ulven and Kostenis, 2005). However, the inability of ramatroban to selectively inhibit one receptor to the exclusion of the other currently precludes our ability to draw any clear inferences from in vivo studies conducted with this molecule. Hence, potent and selective CRTH2 antagonists would be desirable to explore the involvement of PGD2 and CRTH2 in allergic and atopic conditions.

Antagonists of G protein-coupled receptors can be distin-guished as either surmountable or insurmountable (Lew et al., 2000; Vauquelin et al., 2002). Surmountable antagonists produce parallel rightward shifts of agonist concentration-response curves without altering the maximal agonist response. Insurmountable antagonists partially or completely decrease the maximal agonist response and may or may not induce concomitant rightward shifts of agonist dose-response curves. Insurmountable antagonism has been observed for a variety of GPCR systems, including those for angiotensin II, histamine, acetylcholine, serotonin, substance P, bradykinin, cysteinyl-leukotrienes, ADP, glutamate, and anaphylatoxin C5a (Schambye et al., 1994; Aramori et al., 1997; Lew et al., 2000; Carroll et al., 2001; Gillard et al., 2002; Vauquelin et al., 2002; Marteau et al., 2003; Rashid et al., 2003; March et al., 2004; Takezako et al., 2004). It is a priori unclear whether one type of antagonism is desired over the other to obtain clinical efficacy; nevertheless, insurmountable behavior of antagonists may be a means to obtain long-lasting receptor blockade in vivo.

We have previously reported the synthesis and selectivity profile of three novel ramatroban analogs (Fig. 1), which represented the first highly selective and potent CRTH2 antagonists (Ulven and Kostenis, 2005). In the current study, we present a detailed pharmacological analysis of their antagonistic profile, in comparison with ramatroban as a reference antagonist, using mammalian cells overexpressing CRTH2 or human eosinophils that naturally express CRTH2. Despite their close structural resemblance and similar binding affinities to CRTH2, the compounds display significant differences in the nature of their antagonism. Elucidation of the molecular mechanism underlying the divergent modes of CRTH2 blockade (surmountable versus insurmountable) of the compounds is presented. This is the first report disclosing both surmountable and insurmountable selective and potent antagonists for CRTH2 as valuable tools for further exploring the role of CRTH2 in vitro and in vivo.

Materials and Methods

Materials

White 96-well Optiplates and DeepBlueC were obtained from PerkinElmer Life and Analytical Sciences (Boston, MA). Tissue culture media and reagents were purchased from the Invitrogen (Breda, The Netherlands). PGD2 was from Cayman Chemical (Ann Arbor, MI) and [³H]PGD2 was from PerkinElmer Life and Analytical Sciences. TM27868 was obtained from ChemDiv (San Diego, CA). Eotaxin was from Preprotech EC (London, UK). CellFix and FACS-Flow were from BD Immunocytometry Systems (Vienna, Austria). Fixative solution was prepared by diluting Cellfix 1:10 in distilled water and 1:4 in FACSFlow. Ramatroban was obtained from Bayer AG (Wuppertal, Germany). Synthesis of the CRTH2 antagonists TM30642, TM30643, and TM30089 was described previously (Ulven and Kostenis, 2005). All other laboratory reagents were from Sigma-Aldrich (St. Louis, MO), unless explicitly specified.

Generation/Origin of the cDNA Constructs

The coding sequence of human CRTH2 (GenBank accession no. NM_004778) was amplified by PCR from a human hippocampus cDNA library and inserted into the pcDNA3.1(+) expression vector (Invitrogen) via 5' HindIII and 3' EcoRI. To generate a CRTH2-*Renilla reniformis* luciferase (CRTH2-Rluc) fusion protein, the CRTH2 coding sequence without a STOP codon and Rluc were amplified, fused in frame by PCR, and subcloned into the pcDNA3.1(+)Zeo expression vector. For ELISA experiments, the 78-
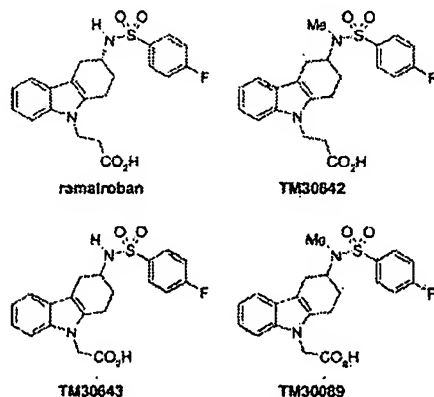

Fig. 1. Structures of ramatroban and its analogs TM30642, TM30643, and TM30089.

base pair M1 FLAG-epitope tag was introduced by PCR at the extreme N terminus, and the resulting construct was inserted via 5′ NheI and 3′ EcoRI into pcDNA3.1(+). Human β-arrestin2 (β-arr2) N-terminally tagged with GFP² (GFP²/β-arr2) and *R. reniformis* luciferase were purchased from Packard BioSignal Inc. The β-arr2 mutant incapable of interacting with the endocytic machinery (β-arr2, R393E, R395E) was a generous gift from R. Jørgensen (7TM Pharma A/S, Hørsholm, Denmark) and has been described previously (Vrecl et al., 2004). The sequence identity of the constructs was verified by restriction endonuclease digests and sequencing in both directions on an ABI Prism 310 DNA sequencer (Applied Biosystems, Foster City, CA).

Cell Culture and Transfection

COS-7 cells were grown in Dulbecco's modified Eagle's medium 1885 supplemented with 10% fetal bovine serum and 10 μg/ml gentamicin and kept at 37°C in a 10% CO_2 atmosphere. HEK293 cells were maintained in minimal essential medium supplemented with 10% (v/v) heat-inactivated fetal calf serum, 2 mM GlutaMAX-I, 1% nonessential amino acids, 1% sodium pyruvate, and 10 μg/ml gentamicin. For functional inositol phosphate assays, COS-7 cells were transiently cotransfected with CRTH2 and a promiscuous $G\alpha$ protein facilitating inositol phosphate production by the G_i-selective CRTH2 receptor (Kostenis et al., 2005) using a calcium phosphate-DNA coprecipitation method with the addition of chloroquine (Mathiesen et al., 2005). To perform the functional bioluminescence resonance energy transfer (BRET) assays, a HEK293 cell clone stably expressing βarr2-R393E, R395E-GFP², and CRTH2-Rluc was generated. This cell line will hereafter be referred to as CRTH2-HEK293 stable cells.

Binding Experiments

Whole Cell Binding. CRTH2-HEK293 cells were seeded into 96-well plates at a density of 30,000 cells/well. Competition binding experiments on whole cells were then performed approximately 18 to 24 h later using 1.2 nM [³H]PGD2 (172 Ci/mmol; NEN) in a binding buffer consisting of HBSS (Invitrogen) and 10 mM HEPES, pH 7.4. Competing ligands were diluted in DMSO, which was kept constant at 1% (v/v) of the final incubation volume. Total and nonspecific binding were determined in the absence and presence of 10 μM PGD2. Binding reactions were routinely conducted for 3 h at 4°C and terminated by two washes (100 μl each) with ice-cold binding buffer. Radioactivity was determined by liquid scintillation counting in a TopCount liquid scintillation counter (PerkinElmer Life and Analytical Sciences) after overnight incubation in MicroScint 20. For saturation binding experiments, CRTH2-HEK293 cells were incubated with 1.5 to 48 nM [³H]PGD2 for 3 h in the absence and presence of equivalent concentrations (with respect to receptor occupancy) of CRTH2 antagonists, and nonspecific binding determined in the presence of 10 μM PGD2. The exact concentration of [³H]PGD2 used was determined from experiment to experiment. Determinations were made in duplicates.

Dissociation Kinetics. CRTH2-HEK293 whole cells (250,000 cells/ml) were incubated at 4°C with 3 nM [³H]PGD2 in binding buffer (HBSS + 10 mM HEPES, pH 7.4) for 60 min to obtain equilibrium. Dissociation was initiated by adding 10 μM PGD2 alone or in combination with 20 μM CRTH2 antagonists ramatroban, TM30089, or TM27868, respectively. After various time intervals, 200-μl aliquot samples were taken, and the reaction was terminated by sample filtration on a Millipore vacuum manifold using Whatman GF/F filters (presoaked in 0.5% BSA for at least 1 h). The filters were washed rapidly three times with 3 ml of ice-cold binding buffer, and radioactivity was determined in a beta counter (PerkinElmer Life and Analytical Sciences). In a separate set of dissociation kinetics, dissociation was initiated with an excess of PGD2 (10 μM), ramatroban (20 μM), or TM30089 (20 μM) alone.

Association Kinetics. The rate of [³H]PGD2 binding to CRTH2 receptors in whole CRTH2-HEK293 cells at 4°C was measured after preincubation with vehicle (DMSO) or equivalent concentrations of CRTH2 antagonists (K_i × 10) for 30 min. CRTH2-HEK293 whole cells were preincubated with antagonists or vehicle for 30 min, washed in 10 ml of binding buffer to remove nonbound antagonist, and resuspended, followed by addition of 4 nM [³H]PGD2 to initiate association using 500,000 cells/ml. After various time intervals, 200-μl aliquot samples (100,000 cells) were taken and processed as described under *Dissociation Kinetics*. Binding equilibrium was reached after 60 min at 4°C.

BRET² Assay

Functional BRET² (hereafter referred to as BRET) assays were performed on HEK293 cells stably expressing human CRTH2-Rluc and GFP²-β-arr2, R393E, R395E essentially as described previously (Vrecl et al., 2004). Before the assay, cells were detached and resuspended in Dulbecco's PBS with 1000 mg/l L-glucose at a density of $2 × 10^6$ cells/ml. DeepBlueC was diluted to 50 μM in Dulbecco's PBS with 1000 mg/l L-glucose (light sensitive). Cell suspension (100 μl) was transferred to wells in a 96-well microplate (white OptiPlate) and placed in the Mithras LB 940 instrument (Berthold Technologies, Bad Wildbad, Germany). Agonist (12 μl/well) was then injected by injector 1, and 10 μl/well DeepBlueC was injected simultaneously by injector 2. Five seconds after the injections, the light output from the well was measured sequentially at 400 and 515 nm, and the BRET signal [milliBRET (mBRET) ratio] was calculated by the ratio of the fluorescence emitted by GFP²-β-arr2 (515 nm) over the light emitted by the receptor-Rluc (400 nm). Antagonists were preincubated with the cells for 15 min before the addition of agonist and DeepBlueC. Compounds were dissolved in DMSO, and the final DMSO concentration was kept constant at 1% in the assay. For BRET experiments in the presence of pertussis toxin, cells were incubated overnight in the presence of the toxin at a final concentration of 100 ng/ml. Use of the BRET² assay and the GFP²-β-arr2, R393E, R395E mutant for BRET² requires a license from 7TM Pharma A/S.

[³⁵S]GTPγS Binding Assays

Scintillation proximity assay [³⁵S]GTPγS binding was performed on membranes from CHO-K1 cells stably expressing CRTH2 essentially as described in Mathiesen et al. (2005). Four micrograms of membrane protein was incubated in GTPγS binding buffer (50 mM HEPES, pH 7.5, 100 mM NaCl, 5 mM $MgCl_2$, 0.1% BSA, and 10 μg/ml saponin) with 50 nCi of [³⁵S]GTPγS, 1 μM GDP, and 0.4 mg of wheat germ agglutinin-coupled scintillation proximity assay beads (RPNQ0001; GE Healthcare, Little Chalfont, Buckinghamshire, UK) with or without increasing concentrations of PGD2 in the absence or presence of the various CRTH2 antagonists. Parallel assays containing 100 μM nonradioactive GTPγS defined nonspecific binding. Samples were incubated for 30 min at ambient temperature on a plate shaker, centrifuged for 5 min, and radioactivity was counted in a TopCount liquid scintillation counter.

Inositol Phosphate Accumulation Assays

Twenty-four hours after transfection cells were seeded in 24-well tissue culture plates and loaded with 5 μCi of [2-³H]myo-inositol (TRK911; Amersham Biosciences). The next day, cells were washed twice in HBSS buffer (including $CaCl_2$ and $MgCl_2$; Invitrogen) and stimulated with the respective agonists in HBSS buffer supplemented with 5 mM LiCl for 45 min at 37°C. Antagonists are routinely preincubated for 15 min before the 45-min agonist incubation period. The reactions were terminated by aspiration and addition of 10 mM ice-cold formic acid and incubated for 30 min on ice. The lysate was applied to AG 1-X8 anion exchange resin (Bio-Rad, Hercules, CA) and washed twice with buffer containing 60 mM sodium formate and 5 mM borax. The [³H]inositol phosphate fraction was

then eluted by adding 1 M ammonium formate and 100 mM formic acid solution and counted after addition of HiSafe3 scintillation fluid (PerkinElmer Life and Analytical Sciences).

Enzyme-Linked Immunosorbent Assay

Determination of cell surface expression levels of CRTH2 was performed using an N-terminally FLAG-tagged CRTH2 receptor in an ELISA assay as described previously (Mathiesen et al., 2005). Twenty-four hours after transfection cells were seeded in poly-D-lysine-coated 48-well tissue culture plates at a density of 100,000 cells/well. Approximately 48 h after transfection, cells were washed once in minimal essential medium + 0.1% BSA and exposed to the indicated compounds diluted in the same buffer for 30 or 180 min at both 37 and 4°C. Cells were then fixed with 4% paraformaldehyde, and CRTH2 surface expression levels were determined with the 3,3',5,5'-tetramethylbenzidine (Sigma-Aldrich) substrate. All experiments were performed in triplicate determinations.

Human Eosinophil Shape Change Assay

Blood was sampled from healthy volunteers according to a protocol approved by the Ethics Committee of the University of Graz and processed as described previously (Bohm et al., 2004). Preparations of polymorphonuclear leukocytes (containing eosinophils and neutrophils) were prepared by dextran sedimentation of citrated whole blood and Histopaque gradients. The resulting cells were washed and resuspended in assay buffer (comprising PBS with Ca^{2+}/Mg^{2+} supplemented with 0.1% BSA, 10 mM HEPES, and 10 mM glucose, pH 7.4) at 5×10^6 cells/ml. Cells were incubated with the antagonists or vehicle (PBS or DMSO) for 10 min at 37°C and then stimulated with various concentrations of the agonists (PGD2 or eotaxin) for 4 min at 37°C. To stop the reaction, samples were transferred to ice and fixed with 250 μl of fixative solution. Samples were immediately analyzed on a FACSCalibur flow cytometer (BD Biosciences), and eosinophils were identified according to their autofluorescence in the FL-1 and FL-2 channels. Shape change responses were quantified as percentage of the maximal response to PGD2 or eotaxin in the absence of an antagonist.

Calculations and Data Analysis

Analysis was performed using Prism 4.03 (GraphPad Software Inc., San Diego, CA). Data sets of saturation binding isotherms were analyzed via nonlinear regression according to a hyperbolic, one-site binding model, and individual estimates for total receptor number (B_{max}) and radioligand dissociation constant (K_A) were calculated. The following equation was used:

$$Y = \frac{B_{max} \cdot [A]}{K_A + [A]} \quad (1)$$

where [A] denotes the concentration of radioligand, and B_{max} and K_A denote the true PGD_2 binding capacity and affinity, respectively.

Specific binding data from the [³H]PGD2 competition binding assays using the test antagonists were normalized and fitted to the following empirical one-site model for competitive interaction:

$$Y = Bottom + \frac{(Top - Bottom)}{1 + \frac{[B]}{K_B\left(1 + \frac{[A]}{K_A}\right)}} \quad (2)$$

where Y denotes percentage of specific binding, Top denotes maximal asymptotic binding, Bottom denotes the minimal asymptotic binding, [A] denotes the concentration of radioligand, [B] denotes the concentration of inhibitor, and K_A and K_B denote their respective equilibrium dissociation constants.

Data sets of [³H]PGD2 homologous competition binding experiments (total binding), performed in the absence or presence of increasing concentrations of each test antagonist, were initially globally fitted to the following model for simple homologous competition:

$$Y = \frac{B_{max} \cdot [A_{Hot}]}{[A_{Hot}] + [A_{Cold}] + K_A} + NS \quad (3)$$

where B_{max} denotes the apparent maximal density of binding sites, K_A denotes the apparent equilibrium dissociation constant of PGD_2, $[A_{Hot}]$ denotes the concentration of radioligand, $[A_{Cold}]$ denotes the concentration of unlabeled PDG_2 (the independent variable), and NS denotes the fraction of nonspecific binding (Motulsky and Christopoulos, 2004). Note that the estimates of B_{max} and K_A are only estimates of true PGD_2 binding capacity and affinity, respectively, for the control curve in the absence of added antagonist. Subsequent to this fit, an F-test was used to determine whether the data could be better fitted by sharing the B_{max} and estimating a separate K_A for each curve (consistent with the expectations of competitive antagonism) or by sharing the K_A across the curves and estimating a separate B_{max} for each curve (indicative of noncompetitive antagonism; see Fig. 4 under *Results* for example). Data sets that were better described by assuming no change in B_{max} with increasing antagonist concentrations were then globally fitted to the following homologous binding model, which explicitly describes a surmountable competitive interaction between radioligand, homologous displacer and a second antagonist:

$$Y = \frac{B_{max} \cdot [A_{Hot}]}{[A_{Hot}] + [A_{Cold}] + K_A\left(1 + \frac{[B]}{K_B}\right)} + NS \quad (4)$$

where [B] denotes the concentration of second antagonist, K_B denotes its equilibrium dissociation constant, and all other parameters are as described above. In contrast, data sets that were better described by assuming no change in K_A with increasing antagonist concentrations were then globally fitted to the following homologous binding model, which explicitly describes an insurmountable noncompetitive interaction between radioligand, homologous displacer and a second antagonist

$$Y = \frac{B_{max} \cdot \left(\frac{K_B}{[B] + K_B}\right) \cdot [A_{Hot}]}{[A_{Hot}] + [A_{Cold}] + K_A} + NS \quad (5)$$

Functional concentration-response curves for PGD2 obtained in the absence or presence of CRTH2 antagonists were fitted via nonlinear regression analysis to the following four-parameter logistic equation:

$$Y = \frac{(Top - Bottom)}{1 + 10^{(\log(EC_{50}) - \log[A])n_H}} + Bottom \quad (6)$$

where Top denotes maximal asymptotic binding, Bottom denotes the minimal asymptotic binding, [A] denotes the concentration of radioligand, and and n_H is the Hill coefficient. EC_{50} values were obtained as a measure of agonist potency and represent the effective concentrations of half-maximal responses.

pA_2 values were estimated from dose ratios (DR) calculated from the EC_{50} values of the individual dose response curves obtained in the absence ($EC_{50,agonist\ alone}$) and presence ($EC_{50,+[B]}$) of CRTH2 antagonists by fitting to the following equation using linear regression:

$$\log\left(\frac{EC_{50,+[B]}}{EC_{50,agonist\ alone}}\right) = \log([B]) - \log(K_B) \quad (7)$$

where [B] denotes the antagonist concentration used when estimating the EC_{50} for the agonist, and K_B is the dissociation constant of the antagonist. pA_2 was estimated as the interception of the regression line with the x-axis.

Data from association and dissociation kinetic experiments were analyzed to calculate the dissociation rate constants (K_{-1}) and the

observed association rate constants (K_{app}). To determine the dissociation rate constants of PGD2, data were fitted by nonlinear regression to the following equation:

$$Y = Y_{max} \cdot e^{-K_{-1} \cdot t} \qquad (8)$$

where K_{-1} is the dissociation rate constant, and Y_{max} denotes the amount of specific binding at 0 min.

To determine the apparent association rate constant of PGD2 data were fitted by nonlinear regression to the following equation representing a biphasic association process:

$$Y = Y_{max1} \cdot (1 - e^{-K_{app1} \cdot t}) + Y_{max2} \cdot (1 - e^{-K_{app2} \cdot t}) \qquad (9)$$

where the curve ascends to $Y_{max1} + Y_{max2}$ via a biphasic exponential association; K_{app1} and K_{app2} denote the individual apparent association rate constants.

In practice, all estimates of ligand potency or affinity were obtained as logarithms.

Results

The Tetrahydrocarbazoles TM30642, TM30643, and TM30089 Are Almost Equipotent Inhibitors of [³H]PGD2 Binding at Human CRTH2 Receptors

At the outset, ramatroban and the three analogs were tested for their ability to compete for [³H]PGD2 specific binding to human CRTH2 receptors stably expressed in HEK293 cells (CRTH2-HEK293 cells). All three compounds displaced [³H]PGD2-specific binding concentration dependently (Fig. 2) with estimated antagonist dissociation constants as shown in Table 1. The affinity of the reference antagonist ramatroban as determined in this set of assays is congruent with previously reported data (Sugimoto et al., 2003; Ulven and Kostenis, 2005; Fig. 2). To characterize the effects of the compounds on [³H]PGD2 binding in more detail, [³H]PGD2 saturation isotherms were generated in the absence and presence of equivalent concentrations (with respect to receptor occupancy) of inhibitor compounds (approx. $3 \times K_i$) (Fig. 3A). Compounds interacting with a receptor in a competitive and reversible manner alter radioligand affinity without affecting ligand binding capacity (B_{max}). Conversely, compounds interacting in a noncompetitive, slowly reversible or irreversible manner reduce binding capacity but have minimal, or no, effect on the affinity of the radiotracer. In the absence of competitor compounds, [³H]PGD2 binding to CRTH2-HEK293 whole cells was saturable, and data were fitted adequately to a one-site binding model [eq. 1; equilib-
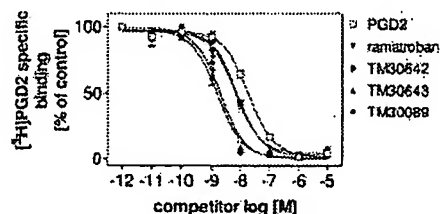

Fig. 2. Affinities of ramatroban and the three analogs TM30642, TM30643, and TM30089 for the cloned human CRTH2 receptor stably expressed in HEK293 cells (CRTH2-HEK293 cells). CRTH2-HEK293 whole cells were incubated at 4°C for 3 h with increasing concentrations of the competitor compounds. Nonspecific binding was defined in the presence of 10 μM PGD2. K_i values were calculated by transforming the IC_{50} values according to the Cheng-Prusoff equation as described under *Materials and Methods*. Symbols represent the mean ± S.E. of three independent experiments conducted in duplicate.

rium dissociation constant (K_D) and B_{max} values amounted to $K_D = 11.1 \pm 2.7$ nM, $B_{max} = 3.1 \pm 0.6$ pmol/mg]. To better visualize the apparent effects of the compounds on [³H]PGD2 affinity and receptor number, Scatchard plots were derived from the saturation isotherms (Fig. 3B). In the presence of ramatroban and its N-methylated analog TM30642 the affinity of [³H]PGD2 seemed to decrease as indicated by flatter slopes of the Scatchard regression lines, whereas B_{max} values remained unaffected as shown by similar interceptions of regression lines with the x-axis (Fig. 3B). In contrast, incubation of CRTH2-HEK293 cells with TM30643 and TM30089, in which the side chain linking the tetrahydrocarbazole scaffold with the carboxylic acid moiety is shortened by one methylene unit, seemed to decrease the number of PGD2 binding sites but did not alter PGD2 affinity.

Although saturation binding experiments and Scatchard analysis indicated a reduced [³H]PGD2 binding capacity in the presence of TM30643 and TM30089, a rigorous test of this assumption would have required a larger range of antagonist concentrations, and, as a consequence, appreciably larger (and practically unobtainable) tracer concentrations. In an attempt to circumvent this limitation but retain an ability to reliably quantify antagonist effects on radioligand binding affinity versus binding capacity, we developed a novel analytical method that is described in detail under *Materials and Methods*. To this end, a series of [³H]PGD2 homologous competition binding experiments were performed in the absence and presence of increasing concentrations of the respective CRTH2 antagonists. As shown in Fig. 4, a global analysis of the data according to eq. 3 under *Materials and Methods*, followed by F-test, revealed that the interaction between PGD2 and either ramatroban or TM30642 was best fitted by a model that assumed a change in the apparent affinity of PGD2 with no change in PGD2 B_{max}; a single best-estimate of the latter parameter was able to describe all the curves in the data set for each antagonist. This behavior is consistent with simple surmountable antagonism. In contrast, application of the same test to the data measuring the interaction between PGD2 and either TM0643 or TM30089 revealed that the entire family of curves could best be fitted by assuming no change in PGD2 affinity (described by a single estimate for $\log K_A$) but a progressive reduction in B_{max} with increasing antagonist concentra-

TABLE 1

Antagonist potency estimates ($-\log K_B$ values) for indole CRTH2 antagonists determined from radioligand binding assays

Values are the mean of three to five independent experiments performed in duplicate. Unpaired t tests showed that TM30643 and TM30089 had significantly higher affinity to the receptor than ramatroban and 30642, respectively ($p < 0.01$) in both radioligand binding assays.

Compound	Assay	
	[³H]PGD2 Inhibition Binding	[³H]PGD2 Homologous Competition Binding
Ramatroban	8.19 ± 0.06[a]	8.13 ± 0.01[b]
TM30642	8.15 ± 0.07[a]	8.35 ± 0.03[b]
TM30643	8.85 ± 0.06[a]	8.89 ± 0.04[c]
TM30089	8.74 ± 0.09[a]	8.93 ± 0.05[c]

[a] Parameter estimates represent the negative logarithm of the antagonist dissociation constant, derived by nonlinear regression analysis according to a competitive model (eq. 2).

[b] Negative logarithm of the antagonist dissociation constant, derived by global nonlinear regression analysis according to a competitive binding model (eq. 4).

[c] Negative logarithm of the antagonist dissociation constant, derived by global nonlinear regression analysis according to a noncompetitive binding model (eq. 5).

tion—behavior that is consistent with insurmountable antagonism. As a consequence, the ramatroban and TM30642 data sets were refitted to eq. 4 under *Materials and Methods*, which is based on a competitive model of interaction, to explicitly estimate the dissociation constant for either antagonist when interacting with PGD2; the resulting values are shown in Table 1. In contrast, the TM30643 or TM30089 data sets were globally refitted to eq. 5 under *Materials and Methods*, which is based on the standard model for noncompetitive antagonism. The estimated affinity values for these latter two antagonists are also shown in Table 1. It is noteworthy that a comparison of the antagonist affinity estimates obtained by this approach with those obtained by the more traditional inhibition binding method (Fig. 2), which assumes a strictly competitive, surmountable antagonism between ligands, yielded very similar values. An explanation as

to why this may be so is outlined under *Discussion* and the Appendix. Together, the inhibition and saturation binding experiments revealed that the tetrahydrocarbazole CRTH2 antagonists display similar receptor binding affinities but belong to two different pharmacological classes (i.e., surmountable and insurmountable antagonists).

Effects of the Compounds on PGD2-Mediated Responses in Different Functional Assays in Mammalian Cells, Overexpressing CRTH2

To determine the functional consequences of the divergent effects on [^{3}H]PGD2 binding, concentration-dependent inhibition of PGD2 responses by the CRTH2 antagonists was evaluated in a set of different functional assays. We were particularly curious about the nature of antagonism of TM30643 and TM30089, because both compounds clearly
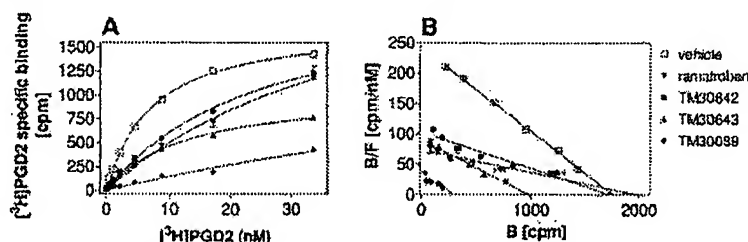

Fig. 3. Effect of ramatroban, TM30642, TM30643, and TM30089 on [^{3}H]PGD2 saturation binding in CRTH2-HEK293 cells. A, representative saturation analysis of [^{3}H]PGD2 binding to CRTH2 receptors in whole cells in the absence or presence of equivalent concentrations (with respect to receptor occupancy) of the compounds. Concentrations of compounds chosen inhibited approximately 75% of [^{3}H]PGD2 specific binding at equilibrium (approximately 30 × K_i; see Fig. 2). Data were fitted best to a one-binding site model, and K_D and B_{max} values were determined. B, Scatchard transformation of the saturation isotherms shown in A. TM30643 and TM30089 significantly lowered B_{max} ($p < 0.05$) compared with vehicle- and ramatroban/TM30642-treated cells. [^{3}H]PGD2 K_D values were significantly higher ($p < 0.05$) in the presence of ramatroban and TM30642 compared with vehicle-treated cells.
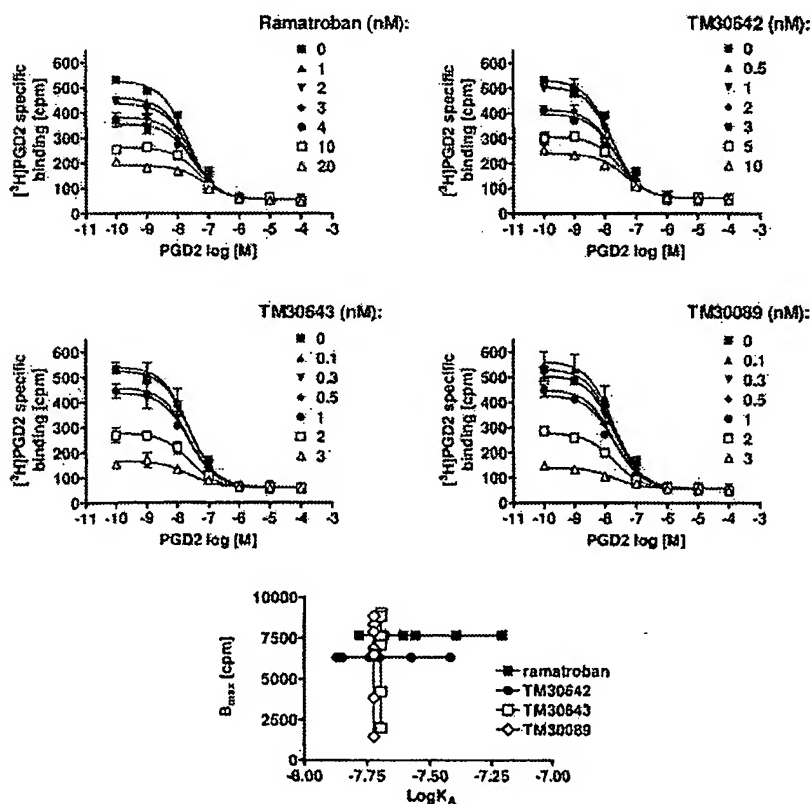

Fig. 4. Homologous competition binding between [^{3}H]PGD2 (1.2 nM) and unlabeled PGD2 in the absence or presence of the indicated concentrations of CRTH2 antagonist. The data for ramatroban and TM30642 represent the best global fit according to a competitive binding model where the effect of each antagonist is to reduce the apparent binding affinity of PGD2 with no effect on the B_{max} (as determined by F-test). The data for TM30643 and TM30089 represent the best global fit according to a noncompetitive binding model, where the effect of each antagonist is to reduce the B_{max} of PGD2 with no effect on its binding affinity (as determined by F-test). Also shown is the relationship between the best-fit values for apparent B_{max} and $\log K_A$ for each data set. Data shown are representative of a single experiment, performed in duplicate, which was repeated five times.

reduced the available number of PGD2 sites on the cell surface, which may correlate to insurmountable inhibition of agonist responses in functional assays. First, the compounds were tested for their ability to antagonize PGD2-mediated stimulation of [^{35}S]GTPγS binding in membrane preparations from stably transfected CRTH2 cells (Fig. 5). Ramatroban and TM30642 caused parallel rightward shifts of the PGD2 concentration-response curves without altering the maximal PGD2 response, consistent with competitive and reversible antagonism. Estimated pA_2 values and slopes of the Schild regressions amounted to pA_2 = 7.44 ± 0.14, n_H = 0.91 ± 0.05 (n = 5) for ramatroban, and pA_2 = 7.72 ± 0.13, n_H = 0.89 ± 0.075 (n = 3) for TM30642, respectively. In contrast, TM30089 simultaneously shifted the PGD2 dose-response curve to the right and decreased the maximal PGD2 response, indicating insurmountable antagonism. TM30643 induced clear rightward shifts of PGD2 concentration-effect curves in concentrations up to 1 μM; at a concentration of 10 μM, however, E_{max} of PGD2 seemed to be depressed. A pA_2 value for TM30643 was computed excluding the PGD2 dose-response curve in the presence of the highest applied concen-
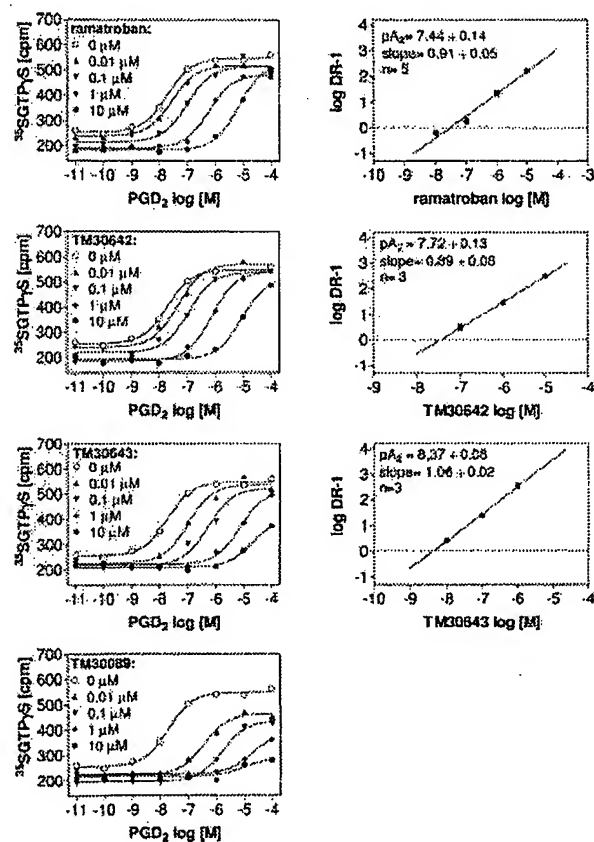
tration of TM30643 and amounted to pA_2 = 8.37 ± 0.08, n_H = 1.06 ± 0.02 (n = 3).

Very similar pharmacological profiles of the antagonists were obtained when inhibition of PGD2-stimulated inositol phosphate production (Supplemental Fig. 1) or β-arrestin translocation was measured (Fig. 6). It is noteworthy that the level of attenuation of maximal PGD2 responses was greater in inositol phosphate and β-arrestin translocation assays (Fig. 6) compared with GTPγS assays (Fig. 5), which may relate to the lower level of CRTH2 receptor expression in the former two assays (B_{max} = 3.1 versus 10.2 pmol/mg protein). None of the compounds showed any significant stimulatory effect in the various functional assays (Supplemental Fig. 2). Together, the functional data reveal that TM30642 and ramatroban exhibit surmountable inhibition of PGD2 responses, whereas TM30089 and to a lesser extent TM30643 clearly display insurmountable antagonism.

We have recently shown that CRTH2-mediated β-arrestin recruitment has a major G protein-independent component and is uncoupled from $G\alpha_{i/o}$ activation in HEK293 cells (Mathiesen et al., 2005). To test whether the set of CRTH2 antagonists retains its pharmacological profile when β-arrestin recruitment is exclusively mediated in a G protein-inde-

Fig. 5. Effects of ramatroban, TM30642, TM30643, and TM30089 on PGD2-mediated stimulation of [^{35}S]GTPγS binding in Chinese hamster ovary cell membranes stably expressing human CRTH2. PGD2 dose-response curves were performed in the presence of the indicated concentrations of the compounds (left) and dose ratios were transformed into Schild plots (right). The plots of the dose ratios over antagonist concentration were subjected to linear regression analysis, and pA_2 values were determined as the x-intercepts at log (DR − 1) = 0. Data are means ± S.D. of one of three representative experiments each performed in duplicate.
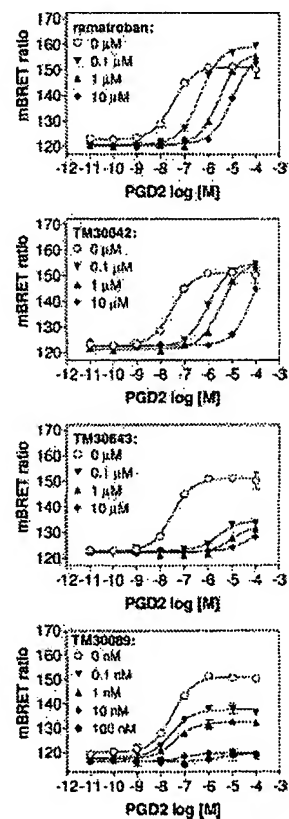

Fig. 6. Effects of ramatroban, TM30642, TM30643, and TM30089 on PGD2-mediated stimulation of β-arrestin recruitment by CRTH2 in BRET assays. HEK293 cells stably transfected with a modified β-arrestin-GFP[2] and CRTH2-Rluc (for details, see *Materials and Methods*) were preincubated for 15 min at 37°C with fixed concentrations of the compounds before arrestin translocation was initiated by addition of increasing concentrations of PGD2. mBRET ratios were calculated as described under *Materials and Methods*. Shown are means ± S.D. of one of three independent experiments, each performed in duplicate.

pendent manner, CRTH2-expressing cells were pretreated with PTX, a selective inhibitor of $G\alpha_{i/o}$ proteins. PTX treatment decreased PGD2-mediated arrestin recruitment in CRTH2-HEK293 cells by approximately 20%, confirming the substantial $G\alpha_i$-independent component. However, the nature of antagonism of the compounds was essentially unchanged in PTX-treated cells (Supplemental Fig. 3), suggesting that the nature of antagonism is independent of the cellular signaling pathway used by CRTH2.

The Compounds Preserve Their Pharmacological Profile in Human Eosinophils, Naturally Expressing CRTH2

It is well known that insurmountable antagonism not only depends on the level of receptor expression in a given tissue or cell but also may differ depending on the cellular environment of a given receptor. We therefore analyzed antagonist behavior in a more natural ex vivo cell system, using human eosinophils, which endogenously express CRTH2 as a model system. Purified human eosinophils undergo shape change upon exposure to PGD2 that is characterized by a biphasic dose-response curve (Hirai et al., 2001; Bohm et al., 2004); the response is known to be mediated via CRTH2, because it is sensitive to blockade with CRTH2 antagonists (Bohm et al., 2004; Mathiesen et al., 2005; Mimura et al., 2005). Our study confirmed the inhibitive effect of ramatroban, which led to concentration-dependent dextral shifts of the PGD2-mediated shape change responses, consistent with classic competitive antagonism (Fig. 7). TM30642 displayed the same antagonistic profile as ramatroban, primarily affecting the high-potency component of the biphasic dose-response curve. In contrast, TM30643 and TM30089 exhibited insurmountable antagonism with clear concentration-dependent suppressions of PGD2 responses, albeit the nature of their insurmountable inhibition seemed to differ in the eosinophil ex vivo system; whereas TM30643 reduces both potency and efficacy of PGD2, TM30089 seems to exclusively reduce the maximum responses of both components. We have previously reported that some aspects of CRTH2 signaling apparently occur independent of G protein activation (Mathiesen et al., 2005) and that both G protein-dependent and -independent signaling account for the characteristic shape change response of human eosinophils exposed to PGD2. Thus, it is conceivable that the antagonists differentially inhibit the two components of the shape change response. At present, however, it is not possible to predict the consequences of such preferential inhibition for interference with eosinophil function in vivo. It is noteworthy that inhibition of PGD2-mediated shape change was specifically mediated through blockade of CRTH2 because neither antagonist interfered with eosinophil shape change elicited by the chemokine eotaxin (CCL11), which acts through the chemokine CCR3 receptor (Supplemental Fig. 4; Bohm et al., 2004).

Molecular Mechanism of Insurmountable Antagonism

Insurmountable Antagonists Do Not Decrease CRTH2 Receptor Cell Surface Expression. To investigate a potential link between insurmountable antagonism and the ability of the compounds to internalize receptors, we analyzed CRTH2 cell surface expression in the absence and presence of different concentrations of antagonists (20, 200, and 2000 nM) in HEK293 cells stably expressing CRTH2. ELISA assays showed that none of the antagonists signifi-

cantly decreased CRTH2 cell surface numbers as opposed to PGD2 (data not shown). This finding together with the effects of the antagonists on [^{3}H]PGD2 B_{max} in saturation and homologous competition binding analyses is congruent with the notion that insurmountability is not merely related to the disappearance of CRTH2 cell surface receptors but that antagonists rather make CRTH2 inaccessible to its agonist PGD2.

Is Insurmountable Antagonism Mediated via an Allosteric Binding Site? To determine whether the insurmountable antagonism of PGD2 by TM30089 and TM30643 observed in the functional assays could be because of the compounds interacting with an allosteric site different from the orthosteric PGD2 binding domain, CRTH2-HEK293 cells were incubated with 3 nM [^{3}H]PGD2 until equilibrium was reached. Subsequently, dissociation of bound radioligand was monitored over time by adding an excess of unlabeled PGD2 (1000 × K_D) to prevent radioligand reassociation, in the
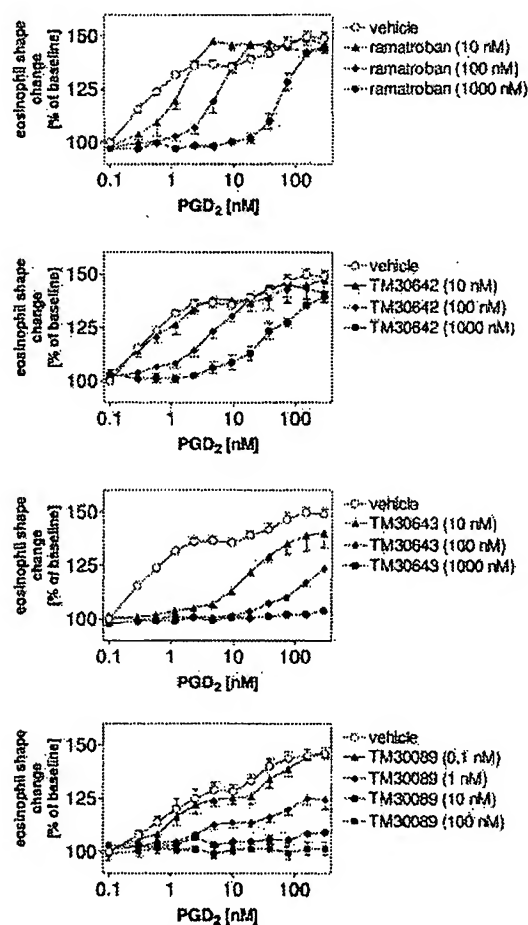

Fig. 7. Inhibition by ramatroban and the analogs TM30642, TM30643, and TM30089 of flow cytometric shape change responses of eosinophils exposed to PGD2. Samples of polymorphonuclear leukocytes were pretreated with the antagonists or their vehicle for 30 min and then stimulated with PGD2. Eosinophils were identified according to their autofluorescence, and shape change responses were quantified as percentage of the maximal response to PGD2 in the absence of an antagonist. Although ramatroban and TM30642 shifted the concentration-response curve to PGD2 rightward in a parallel manner, TM30643 and TM30089 induced both affinity shifts and depression of maximal efficacy of PGD2 dose-response curves. Data are shown as mean ± S.E., $n = 3$.

absence or presence of a high concentration of insurmountable antagonist. If the dissociation rate of [^{3}H]PGD2 is altered by the simultaneous presence of an antagonist, it must be because of antagonist interacting with an allosteric site distinct from the PGD2 binding domain. Figure 8A shows that none of the tested antagonists was capable of affecting the dissociation rate of [^{3}H]PGD2, in contrast to the positive control compound TM27868, which has recently been shown to significantly delay [^{3}H]PGD2 dissociation from CRTH2 receptors (Mathiesen et al., 2005). In another set of kinetic experiments, we tested whether [^{3}H]PGD2 dissociation was differentially affected when monitored only in the presence of excess PGD2, surmountable or insurmountable antagonists. To this end, CRTH2-HEK293 cells were incubated with [^{3}H]PGD2 until equilibrium was reached and dissociation was monitored over time by adding either a large excess of PGD2 (10 μM) or surmountable (20 μM ramatroban) or insurmountable (20 μM TM30089) ligand. Under these experimental conditions, acceleration or retardation of [^{3}H]PGD2 dissociation could be indicative of a cooperative mechanism of binding, whereas dissociation coinciding with that induced by PGD2 would indicate action via the orthosteric site. Dissociation of [^{3}H]PGD2, however, was essentially unchanged when reassociation was precluded by excess PGD2, ramatroban, or TM30089, respectively. Together, the different sets of kinetic experiments clearly support the notion that insurmountability of the antagonists does not arise from cooperative or allosteric interactions with CRTH2, occupation of which may lead to a conformational change refractory to agonist activation.

Relative Rates of Antagonist Dissociation Are Significantly Different for Surmountable and Insurmountable Ligands. To investigate whether insurmountability of TM30643 and TM30089 was related to slow dissociation from CRTH2, an indirect nonequilibrium method was used (Chris-
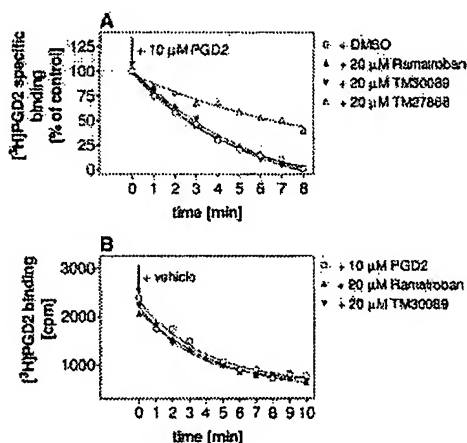
topoulos et al., 1999; Verheijen et al., 2002) because none of the compounds are available in radiolabeled form. The method is based on the assumption that the degree of insurmountability correlates to the rate of antagonist dissociation. First, CRTH2-HEK293 whole cells were pre-exposed for 30 min with equivalent antagonist concentrations ($\sim$10 $\times$ K_i, which corresponds to approximately 90% receptor occupancy) followed by removal of unbound antagonist through a washing procedure. Subsequently, the rate of [^{3}H]PGD2 association was monitored over time (Fig. 9; Table 2). Assuming that the dissociation rate of the unlabeled antagonists will affect the association of the radioligand, apparent [^{3}H]PGD2 association rate constants can be computed to obtain a relative measure of antagonist dissociation. Association curves of [^{3}H]PGD2 in both absence and presence of antagonists were complex and best described by a two-component model (F < 0.05) as is the case for many radioligand agonists, which differentially interact with G protein-coupled and uncoupled forms of the receptor. As depicted in Fig. 9, the initial fast phase K_{app1} of [^{3}H]PGD2 association (K_{app1} = 3.01 $\pm$ 0.76 min^{-1}) ($t_{1/2}$ = 0.231 min; n = 4) was not significantly different across the various antagonist-pretreated groups and most probably reflects association of [^{3}H]PGD2 with the population of free receptors (approximately 10% of the total receptor population is not bound to antagonist at 10 $\times$ K_i). However, the rate constant K_{app2} for the second slower phase of [^{3}H]PGD2 association to the receptor population initially occupied by unlabeled antagonist was differentially affected by surmountable and insurmountable antagonists, respectively. Whereas the surmountable antagonists ramatroban and TM30642 modulated K_{app2} of [^{3}H]PGD2 association only slightly, the insurmountable antagonists TM30643 and TM30089 caused a dramatic reduction of K_{app2} by $\sim$1.5 $\times$ 10^6-fold (Table 2). Thus, the ability of the antagonists to slow [^{3}H]PGD2 association seems to be closely related to their degree of suppression of agonist responses in the functional assays.

Discussion

Approximately 15 years ago, the orally available, small molecule ramatroban was developed as a thromboxane A$_2$ receptor antagonist for clinical use in various cardiovascular, cerebrovascular, and pulmonary diseases, but it has only recently been discovered to also antagonize CRTH2 (Sugi-
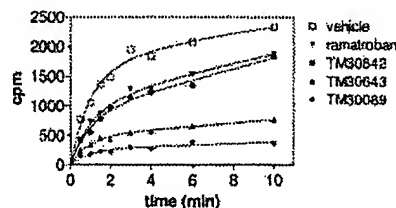
Fig. 8. Time course of [^{3}H]PGD2 dissociation from human CRTH2 receptors stably expressed in HEK293 cells. A, CRTH2-HEK293 whole cells were incubated with 4 nM [^{3}H]PGD2 for 60 min at 4°C until binding equilibrium was attained. Dissociation of [^{3}H]PGD2 was initiated by adding a large excess of PGD2 (10 μM) in the absence or presence of the indicated compounds. Nonspecific binding was determined in the presence of 10 μM PGD2. Binding levels after the initial equilibration phase were set 100% for all dissociation data sets. Shown are representative experiments performed as single point determinations. Two additional experiments gave similar results. B, dissociation was initiated by adding either the surmountable antagonist ramatroban or the insurmountable antagonist TM30089. Shown is a representative experiment.

Fig. 9. Effects of ramatroban, TM30642, TM30643, and TM30089 on [^{3}H]PGD2 association kinetics in CRTH2-HEK293 cells. [^{3}H]PGD2 association kinetics were performed at 4°C in the presence of a single concentration of CRTH2 antagonist (chosen to correspond to K_i $\times$ 10) or their vehicle (control). Cells were pre-exposed to the antagonists for 30 min at 4°C before [^{3}H]PGD2 association was initiated by ligand addition. [^{3}H]PGD2 association curves were analyzed by nonlinear regression analysis using a biexponential model as outlined in detail under *Materials and Methods*. Curves are representative of a single experiment. Four additional experiments gave similar results.

moto et al., 2003). We previously disclosed three ramatroban analogs that differ in structure only slightly from ramatroban (Fig. 1), yet exhibit very weak or no affinity for or functional activity on the thromboxane A_2 receptor, whereas their antagonistic activity on CRTH2 is preserved or potentiated (Ulven and Kostenis, 2005). In this study, we present a detailed pharmacological profile of these compounds and propose receptor binding modes to rationalize the observed pharmacological differences. All compounds inhibited PGD2 binding to CRTH2, but their nature of antagonism differed markedly (surmountable versus insurmountable). We were interested in exploring the molecular mechanisms underlying the experimental observations and also the structural features conferring insurmountability, because this is important from both a basic scientific and drug development point of view.

Proposed mechanisms for insurmountable antagonism include 1) slow dissociation of antagonist-receptor complexes; 2) interaction with allosteric binding sites inducing a conformational change in the receptor that compromises its interaction with the agonist; 3) antagonist-mediated conformational changes rendering receptors refractory to agonist stimulation; 4) antagonist-mediated desensitization or internalization; 5) slow antagonist removal from tissue compartments, cells, or matrix surrounding the receptor; 6) slowly interconverting receptor conformations; and 7) irreversible covalent ligand binding (for review, see Lew et al., 2000, Vauquelin et al., 2002).

Saturation and homologous inhibition binding experiments in the presence of the CRTH2 antagonists performed in this study indicated that TM30643 and TM30089 lead to a decrease of CRTH2 receptors capable of binding ligand; this pattern of behavior is also manifested in the functional effects of these antagonists (Figs. 3–7). It is now well established that receptor desensitization and internalization can occur in the absence of receptor activation (Whistler et al., 2002), and several examples of GPCRs undergoing antagonist-mediated internalization have been described previously (Perry et al., 2005). We therefore investigated whether insurmountable inhibition of PGD2 responses by the ramatroban analogs TM30089 and TM30643 was because of such a property. Although binding analyses indicated that the two insurmountable antagonists significantly depressed B_{max}, ELISA assays (data not shown) revealed that the total number of CRTH2 receptors on the cell surface was not reduced in their presence. Insurmountable antagonism of the compounds is therefore independent of receptor internalization.

To ascertain whether the insurmountability of the com-

pounds reflected a noncompetitive mechanism that was possibly mediated through an allosteric site, [^{3}H]PGD2 dissociation kinetic studies were performed. Occupation by the compounds of an allosteric site may lead to a conformational change of CRTH2 that may perturb its interaction with PGD2 itself and hence its ability to elicit a cellular response. The dissociation kinetics presented in Fig. 8, however, imply that it is unlikely that the insurmountable antagonists interact with an allosteric site, because neither compound altered the rate of [^{3}H]PGD2 dissociation from CRTH2 receptors (Fig. 8A). Furthermore, when dissociation of [^{3}H]PGD2 was monitored in the presence of excess PGD2, ramatroban, or TM30089 alone, the [^{3}H]PGD2 dissociation curves coincided for all three ligands, again suggesting interaction with a common binding site (Fig. 8B). Allosterically acting compounds, on the other hand, could have caused an acceleration or retardation of radioligand dissociation under these conditions because of cooperative binding.

Another possible explanation for insurmountability of orthosteric antagonists is the longevity of antagonist-receptor complexes caused by slow dissociation of antagonists from the receptors (Lew et al., 2000; Vauquelin et al., 2002). As outlined in the Appendix, binding behavior that is consistent with that observed in our current study can arise when the kinetics of one orthosteric ligand in the presence of another are so slow that insufficient readjustment of receptor occupancy occurs over the time course of the experiment. This phenomenon has previously been described as the "hemi-equilibrium" condition (Paton and Rang, 1966; Kenakin, 1997). Because a true state of equilibrium may not be practically reached during the course of such an experiment, affinity estimates for the antagonists have to be obtained under nonequilibrium conditions and hence are likely to deviate from the true affinities of the antagonists. However, as outlined in the Appendix, use of very low radioligand concentrations relative to its dissociation constant is a means to circumvent this problem. In fact, the lower the radioligand concentration used for competition binding assays, the closer will the apparent estimate of orthosteric antagonist affinity approach its true affinity, irrespective of whether antagonism is surmountable or insurmountable (shown by curve simulations in the Appendix). It is clear, however, that the drawback of using low radioligand concentrations is the introduction of uncertainty to the data because of a potentially low signal-to-noise ratio. In our study (Fig. 2; Table 1), the signal-to-noise ratio at low radioligand concentrations did not

TABLE 2

Rate constants and half-lives for [^{3}H]PGD2 association to CRTH2 receptors in the absence (vehicle) and presence of CRTH2 antagonists

[^{3}H]PGD2 association was measured in whole CRTH2-HEK293 cells pre-exposed for 30 min to vehicle or the various CRTH2 antagonists at equieffective concentrations (10 × K_i). Data were fitted to the equation $Y = Y_{max1} \times (1 - e^{(-K_{app1} \times X)}) + Y_{max2} \times (1 - e^{(-K_{app2} \times X)})$ using Prism 4.03. K_{app1} and K_{app2} denote the rate constants for the first and second phase, respectively, of [^{3}H]PGD2 association. Association data in the presence of the antagonists were best described by keeping K_{app1} constant (K_{app1} amounted to 3.01 ± 0.76 min^{-1} ($t_{1/2}$ = 0.231 min) and was not significantly different across the antagonist-treated groups), while keeping K_{app2} as a variable. Unpaired t tests showed that the K_{app2} values of ramatroban and TM30642 were significantly different from those of TM30643 and TM30089, respectively ($p < 0.0001$). Data are from four independent experiments, one experiment of which is shown in Fig. 9.

Pretreatment with	K_{app2}	$t_{1/2}$	-fold $t_{1/2}$ over Ramatroban
	min^{-1}	min	
Vehicle	0.228 ± 0.04	3.05	
Ramatroban	0.151 ± 0.03	4.60	1
TM30642	0.090 ± 0.02	7.72	1.68
TM30643	$1.027 \times 10^{-7} \pm 0.08 \times 10^{-7}$	6.75×10^6	1.47×10^6
TM30089	$0.975 \times 10^{-7} \pm 0.08 \times 10^{-7}$	7.11×10^6	1.55×10^6

represent an experimental obstacle because binding data were very clean even under these conditions.

To more directly confirm whether the molecular mode of interaction between TM30643 or TM30089 with CRTH2 reflects the formation of a long-lasting ligand-receptor complex, additional kinetic binding assays were performed. Because the CRTH2 antagonists are not available in radiolabeled form at present, we took advantage of an indirect method to quantify antagonist dissociation from CRTH2 receptors (Christopoulos et al., 1999; Verheijen et al., 2002). This method determines the delay of [^{9}H]PGD2 association in the presence of equivalent antagonist concentrations (with respect to receptor occupancy) in washout experiments with antagonist-pretreated cells. It is assumed that the delay of agonist association reflects the dissociation rate of the unlabeled compounds from the receptors such that long-lasting receptor occupancy is correlated to the delay of agonist association. Although the four CRTH2 antagonists have quite similar affinities for CRTH2, they differ strikingly from a kinetic point of view. Whereas the surmountable antagonists ramatroban and TM30642 delay PGD2 association only slightly, the insurmountable ligands markedly decrease agonist association in a manner related to their ability to suppress maximal
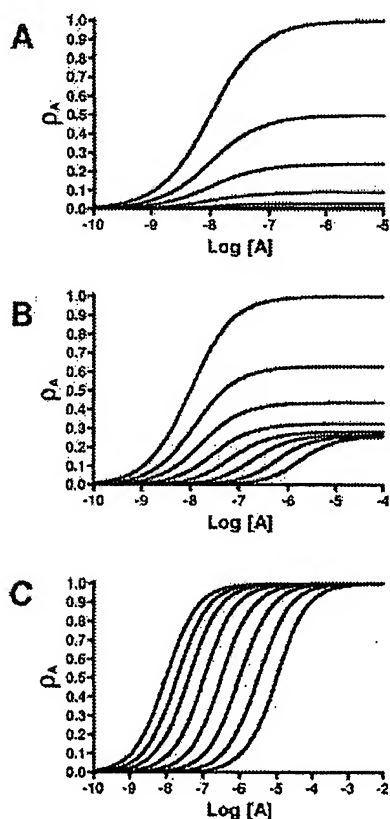

Fig. 10. Simulations of the interaction between an orthosteric ligand, A, in the absence (leftmost curve) or presence of a slowly dissociating orthosteric ligand, B, according to eq. 10. For all simulations, the following parameters were used: $K_A = 10^{-8}$ M, $K_B = 10^{-9}$ M, and $k_{off} = 10^{-4}$ s^{-1}. Concentrations of B ranged from 10^{-9} M to 10^{-7} M in half-log units. The incubation times were 0.5 s (A), 3000 s (B), and 100,000 s (equilibrium) (C). Ordinates, fractional occupancy of ligand A (ρ_A); abscissa, concentration of ligand A.

PGD2 responses in functional assays (Fig. 9; Table 2). It is intriguing to note that compounds whose only structural differences reside in the absence or presence of a methyl group and the absence or presence of a methylene unit in the carboxylic acid chain may display such strikingly different pharmacological profiles. The shorter carboxylic acid chain seems to be associated with insurmountable behavior, whereas the absence or presence of a methyl group at the sulfonamide had no consequence for the kinetic behavior of the compounds. Different modes of antagonism for structurally closely related molecules have also been observed for AT1 receptor antagonists (compare losartan versus its active metabolite EXP3174 (Schambye et al., 1994); or SC-54629 versus SC-54628, which differ only by a single methyl group (Olins et al., 1995); and histamine H1 antagonists [compare (R)- versus (S)-cetirizine; Gillard et al., 2002)].

It is well known that the degree of insurmountable antagonism is related to the level of receptor expression in a given cell. In our study, the extent of depression of maximal PGD2 responses was inversely correlated to receptor expression such that insurmountability was most evident in eosinophil shape change assays with "physiological levels" of receptor expression but least evident in GTPγS assays with very high levels of CRTH2 expression. In addition, we noted a significant discrepancy between the concentrations of insurmountable antagonist required to depress B_{max} in radioligand binding assays and the ability to depress E_{max} in functional assays. This discrepancy was particularly evident for TM30643 and may reflect differences in both receptor reserve but also temperature in binding (4°C) and functional assays (37°C), because binding processes are significantly slower at lower temperatures, leading to apparent overestimation of potency for slowly dissociating ligands.

In conclusion, our study explored in detail the pharmacological profile of three structurally closely related ramatroban analogs that display high potency and selectivity for CRTH2. It also provided insight into the structural features required to elicit insurmountable antagonism and the underlying molecular mechanism showing that slow dissociation from the receptor is sufficient to explain the pharmacological behavior. To date, TM30643 and TM30089 are the only insurmountable CRTH2 antagonists reported in the literature. Yet, it is premature to conclude that slowly dissociating antagonists with the potential to produce long-lasting receptor blockade will be therapeutically advantageous in clinical settings. Although it is clear that many additional pharmacokinetic factors govern duration of compound action in vivo, insurmountability may contribute to this duration and may allow compounds to act much longer as would be predicted from their plasma half-lives.

Appendix

The standard analyses applied to the agonist-antagonist interaction assume that the measured response, be it binding or function, reflects an equilibrium interaction between the ligands. If this assumption is not met by the experimental conditions, complex behaviors can be observed in the data that may lead the investigator to misinterpret the mechanism underlying the interaction. To explore some of the con-

sequences of lack of appropriate equilibrium between two orthosteric ligands, the following equation was used to simulate the re-adjustment in receptor occupancy between an orthosteric ligand, A, exposed to a receptor that has been pre-equilibrated with a second orthosteric ligand, B, as a function of time, t (Paton and Rang, 1966; Kenakin, 1997).

$$
Y = \frac{[A]/K_A}{1 + [A]/K_A} \cdot \left(1 - \left(\left[\frac{[B]/K_B}{1 + [A]/K_A + [B]/K_B}\right]\right.\right.
$$
$$
\cdot \left[1 - e^{-k_{off} \cdot \left[\frac{1 + [A]/K_A + [B]/K_B}{1 + [A]/K_A}\right] \cdot t}\right]
$$
$$
\left.\left. + \frac{[B]/K_B}{1 + [B]/K_B} \cdot e^{-k_{off}\left[1 + \frac{[A]/K_A + [B]/K_B}{1 + [A]/K_A}\right] \cdot t}\right)\right) \quad (A1)
$$

where Y denotes the fractional occupancy of A; K_A and K_B denote the equilibrium dissociation constants of A and B, respectively; and k_{off} denotes the dissociation rate constant of B. Figure 11 illustrates the effects of varying the time of ligand interaction on the occupancy by A. If ligand B has a very low dissociation rate constant (Fig. 10A), it can be seen that at very short exposure times for A, there will be minimal readjustment of receptor occupancy; the occupancy profile of
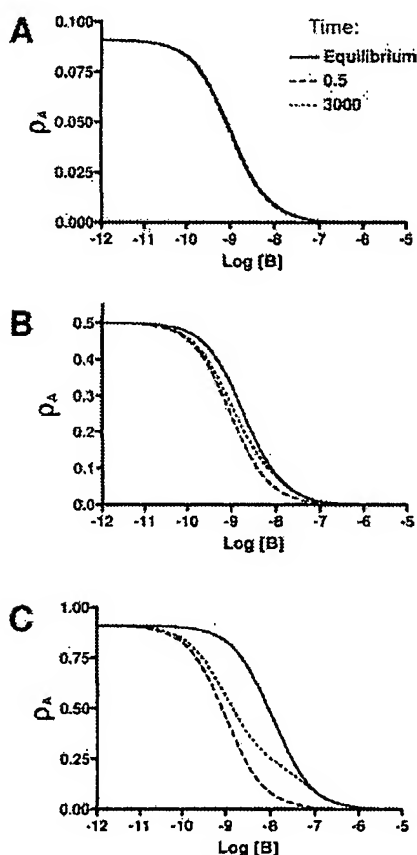

Fig. 11. Simulations of the interaction between a fixed concentration of orthosteric ligand, A, in the absence or presence of increasing concentrations of a slowly dissociating orthosteric ligand, B, according to eq. 10. Parameter values were as described for Fig. 10. Incubation times are indicated in the figure. The concentrations of ligand A were $0.1 \times K_A$ (A), 1 times] K_A (B), or $10 \times K_A$ (C). Ordinates, fractional occupancy of ligand A (p_A); abscissa, concentration of ligand B.

ligand A will essentially reflect its interaction only with the unoccupied receptors. Under this condition, the interaction is indistinguishable from a pure noncompetitive interaction where the effect of the presence of ligand B is to progressively reduce the maximal number of binding sites recognized by ligand A without affecting the affinity of the latter. As the incubation time is increased, a partial re-equilibration occurs that is characterized by a saturable depression in the maximal occupancy of A accompanied by a dextral displacement of the concentration-occupancy curve (Fig. 10B); this has previously been defined as a hemi-equilibrium condition (Paton and Rang, 1966; Kenakin, 1997; Christopoulos et al., 1999). Given sufficient time, complete re-equilibration occurs, and the characteristic features of a simple orthosteric interaction, namely, a parallel dextral shift of the concentration-occupancy curve of A in the presence of B with no effect on the maximal occupancy of A, is observed (Fig. 10C).

A more common method that is used experimentally to monitor the fractional occupancy of one ligand in the presence of another is the inhibition binding assay. Figure 11 shows a series of simulations based on this type of paradigm whereby the concentration of ligand A is held constant, and the effects on its fractional occupancy are monitored as the concentration of ligand B is increased. At a concentration of A that is 10-fold less (Fig. 11A) or equal to (Fig. 11B), its K_A value, it can be seen that no, or minimal, discrepancy occurs in the estimate of the affinity of ligand B. In contrast, at a concentration that is 10 times above the K_A, a dramatic effect of incubation time is evident on the location and shape of the inhibition binding curve. These latter simulations are particularly useful, because they indicate that the most accurate estimates of affinity for a slowly reversible orthosteric ligand are obtained by using as low a concentration as possible of the orthosteric probe ligand.

References

Aramori I, Zenkoh J, Morikawa N, O'Donnell N, Asano M, Nakamura K, Iwami M, Kojo H, and Notsu Y (1997) Novel subtype-selective nonpeptide bradykinin receptor antagonists FR167344 and FR173657. *Mol Pharmacol* 51:171–176.

Bohm E, Sturm GJ, Weiglhofer I, Sandig H, Shichijo M, McNamee A, Pease JE, Kollroser M, Peskar BA, and Heinemann A (2004) 11-Dehydro-thromboxane B2, a stable thromboxane metabolite, is a full agonist of chemoattractant receptor-homologous molecule expressed on TH2 cells (CRTH2) in human eosinophils and basophils. *J Biol Chem* 279:7663–7670.

Boie Y, Sawyer N, Slipetz DM, Metters KM, and Abramovitz M (1995) Molecular cloning and characterization of the human prostanoid DP receptor. *J Biol Chem* 270:18910–18916.

Carroll FY, Stolle A, Beart PM, Voerste A, Brabet I, Mauler F, Joly C, Antonicek H, Bockaert J, Muller T, et al. (2001) BAY36–7620: a potent non-competitive mGlu1 receptor antagonist with inverse agonist activity. *Mol Pharmacol* 59:965–973.

Christopoulos A, Parsons AM, Lew MJ, and El-Fakahany EE (1999) The assessment of antagonist potency under conditions of transient response kinetics. *Eur J Pharmacol* 382:217–227.

Gillard M, Van der PC, Moguilevsky N, Massingham R, and Chatelain P (2002) Binding characteristics of cetirizine and levocetirizine to human h(1) histamine receptors: contribution of Lys(191) and Thr(194). *Mol Pharmacol* 61:391–399.

Gonzalo J, Qiu Y, Coyle AJ, Hodge MR, and Cambridge MA (2005) CRTH2 (DP2), and not the DP1 receptor mediate allergen induced mucus production and airway hyperresponsiveness. The 2005 International Conference of the American Thoracic Society; 2005 May 20–25; San Diego, CA. Poster L41. Available at http://www.abstracts2view.com/ats05/view.php?mu=ATS5L_4220.

Hata AN and Breyer RM (2004) Pharmacology and signaling of prostaglandin receptors: multiple roles in inflammation and immune modulation. *Pharmacol Ther* 103:147–166.

Heinemann A, Schuligoi R, Sabroe I, Hartnell A, and Peskar BA (2003) delta

12-Prostaglandin J2, a plasma metabolite of prostaglandin D2, causes eosinophil mobilization from the bone marrow and primes eosinophils for chemotaxis. *J Immunol* 170:4752–4758.

Hirai H, Tanaka K, Yoshie O, Ogawa K, Kenmotsu K, Takamori Y, Ichimasa M, Sugamura K, Nakamura M, Takano S, et al. (2001) Prostaglandin D2 selectively induces chemotaxis in T helper type 2 cells, eosinophils and basophils via seven-transmembrane receptor CRTH2. *J Exp Med* 193:255–261.

Kenakin TP (1997) *Pharmacologic Analysis of Drug-Receptor Interaction*, 3rd ed, Lippincott-Raven, New York.

Kostenis E, Martini L, Ellis J, Waldhoer M, Heydorn A, Rosenkilde MM, Norregaard PK, Jorgensen R, Whistler JL, and Milligan G (2005) A highly conserved glycine within linker 1 and the extreme C terminus of G protein α subunits interact cooperatively in switching G protein-coupled receptor-to-effector specificity. *J Pharmacol Exp Ther* 313:78–87.

Lew MJ, Ziogas J, and Christopoulos A (2000) Dynamic mechanisms of non-classical antagonism by competitive AT(1) receptor antagonists. *Trends Pharmacol Sci* 21:376–381.

March DR, Proctor LM, Stoermer MJ, Sbaglia R, Abbenante G, Reid RC, Woodruff TM, Wadi K, Paczkowski N, Tyndall JD, et al. (2004) Potent cyclic antagonists of the complement C5a receptor on human polymorphonuclear leukocytes. Relationships between structure and activity. *Mol Pharmacol* 65:868–879.

Marteau F, Le Poul E, Communi D, Communi D, Labouret C, Savi P, Boeynaems JM, and Gonzalez NS (2003) Pharmacological characterization of the human P2Y13 receptor. *Mol Pharmacol* 64:104–112.

Mathiesen JM, Ulven T, Martini L, Gerlach LO, Heinemann A, and Kostenis E (2005) Identification of indole derivatives exclusively interfering with a G protein-independent signaling pathway of the prostaglandin D2 receptor CRTH2. *Mol Pharmacol* 68:393–402.

Mimura H, Ikemura T, Kotera O, Sawada M, Tashiro S, Fuse E, Ueno K, Manabe H, Ohahima E, Karasawa A, et al. (2005) Inhibitory effect of the 4-aminotetrahydroquinoline derivatives, selective chemoattractant receptor-homologous molecule expressed on T helper 2 cell antagonists, on eosinophil migration induced by prostaglandin D2. *J Pharmacol Exp Ther* 314:244–251.

Monneret G, Cossette C, Gravel S, Rokach J, and Powell WS (2003) 15R-Methylprostaglandin D2 is a potent and selective CRTH2/DP2 receptor agonist in human eosinophils. *J Pharmacol Exp Ther* 304:349–355.

Motulsky HJ and Christopoulos A (2004) *Fitting Models to Biological Data Using Linear and Nonlinear Regression. A Practical Guide to Curve Fitting*, Oxford University Press, New York.

Nagata K, Tanaka K, Ogawa K, Kemmotsu K, Imai T, Yoshie O, Abe H, Tada K, Nakamura M, Sugamura K, et al. (1999) Selective expression of a novel surface molecule by human Th2 cells in vivo. *J Immunol* 162:1278–1286.

Olins GM, Chen ST, McMahon EG, Palomo MA, and Reitz DB (1995) Elucidation of the insurmountable nature of an angiotensin receptor antagonist, SC-54629. *Mol Pharmacol* 47:115–120.

Paton WDM and Rang HP (1966) A kinetic approach to the mechanism of drug action. *Adv Drug Res* 3:57–80.

Perry SJ, Junger S, Kohout TA, Hoare SR, Struthers RS, Grigoriadis DE, and Maki RA (2005) Distinct conformations of the corticotropin releasing factor type 1 receptor adopted following agonist and antagonist binding are differentially regulated. *J Biol Chem* 280:11560–11568.

Powell WS (2003) A novel PGD(2) receptor expressed in eosinophils. *Prostaglandins Leukot Essent Fatty Acids* 69:179–185.

Rashid M, Nakazawa M, and Nagatomo T (2003) Insurmountable antagonism of AT-1015, a 5-HT2 antagonist, on serotonin-induced endothelium-dependent relaxation in porcine coronary artery. *J Pharm Pharmacol* 55:827–832.

Rubargo MJ, Bom DC, Tumey LN, Varga N, Gleason E, Silver D, Song J, Murphy SM, Ekema G, Doucette C, et al. (2005) Isosteric ramatroban analogs: selective and potent CRTH-2 antagonists. *Bioorg Med Chem Lett* 15:1749–1753.

Schambye HT, Hjorth SA, Bergsma DJ, Sathe G, and Schwartz TW (1994) Differentiation between binding sites for angiotensin II and nonpeptide antagonists on the angiotensin II type 1 receptors. *Proc Natl Acad Sci USA* 91:7046–7050.

Shiraishi Y, Asano K, Nakajima T, Oguma T, Suzuki Y, Shiomi T, Sayama K, Niimi K, Wakaki M, Kagyo J, et al. (2005) Prostaglandin D2-induced eosinophilic airway inflammation is mediated by CRTH2 receptor. *J Pharmacol Exp Ther* 312:954–960.

Soler D, Frank N, Zhu J, Fedyk E, Rose D, Coyle AJ, Hodge M, and Cambridge MA (2005) CRTH2 activates effector Th2 cell functions independently of antigen stimulation and costimulates proliferative responses via TCR activation. The 2005 International Conference of the American Thoracic Society; 2005 May 20–25; San Diego, CA. Poster L42. Available at http://www.abstracts2view.com/ats05/view.php?nu=ATS5L_4974.

Sugimoto H, Shichijo M, Iino T, Manabe Y, Watanabe A, Shimazaki M, Gantner F, and Bacon KB (2003) An orally bioavailable small molecule antagonist of CRTH2, ramatroban (BAY U3405), inhibits prostaglandin D2-induced eosinophil migration in vitro. *J Pharmacol Exp Ther* 305:347–352.

Takezako T, Gogonea C, Saad Y, Noda K, and Karnik SS (2004) "Network leaning" as a mechanism of insurmountable antagonism of the angiotensin II type 1 receptor by non-peptide antagonists. *J Biol Chem* 279:15248–15257.

Tanaka K, Hirai H, Takano S, Nakamura M, and Nagata K (2004) Effects of prostaglandin D2 on helper T cell functions. *Biochem Biophys Res Commun* 316:1009–1014.

Ulven T and Kostenis E (2005) Minor structural modifications convert the dual TP/CRTH2 antagonist ramatroban into a highly selective and potent CRTH2 antagonist. *J Med Chem* 48:897–900.

Vauquelin G, Van Liefde I, and Vanderheyden P (2002) Models and methods for studying insurmountable antagonism. *Trends Pharmacol Sci* 23:514–518.

Verheijen I, Vanderheyden PM, De Backer JP, Bottari S, and Vauquelin G (2002) Antagonist interaction with endogenous AT(1) receptors in human cell lines. *Biochem Pharmacol* 64:1207–1214.

Vreel M, Jorgensen R, Pogacnik A, and Heding A (2004) Development of a BRET2 screening assay using beta-arrestin 2 mutants. *J Biomol Screen* 9:322–333.

Whistler JL, Gerber BO, Meng EC, Baranski TJ, von Zastrow M, and Bourne HR (2002) Constitutive activation and endocytosis of the complement factor 5a receptor: evidence for multiple activated conformations of a G protein-coupled receptor. *Traffic* 3:866–877.

Address correspondence to: Dr. Evi Kostenis, 7TM Pharma A/S, Fremtidsvej 3, 2970 Hørsholm, Denmark. E-mail: ek@7tm.com

In re the application of

Yoshihiro URADE et al.   Group Art Unit: 1617

Serial No.: 10/520,781   Examiner: JEAN-LOUIS SAMIRA JM

Filed: January 11, 2005
For: DRUGS FOR IMPROVING THE PROGNOSIS
       OF BRAIN INJURY AND A METHOD OF
       SCREENING THE SAME

DECLARATION

Commissioner for Patents
P.O. Box 1450
Alexandria, VA 22313-1450

Sir:

I, Yoshihiro URADE, a citizen of Japan residing at 503, Granshitio-Shimogamo-Shikisaikan, 43, Shimogamo Matsubara-cho, Sakyou-ku Kyoto-shi, kyoto-fu, Japan, declare and say that:

1.   I was graduated from University of Osaka Prefecture in 1978 and went on to the graduate school of Medicine, Kyoto University and took Ph.D. in biochemistry. After that, I was Senior Scientist of Hayaishi Bioinformation Transfer Project, Exploratory Research for Advanced Technology, Research Development Corporation of Japan (1983–87), Senior Scientist of Department of Enzyme and Metabolism, Osaka Bioscience Institute (1987–88), Visiting Professor of Roche Institute of Molecular Biology (1988–90), Senior Scientist of International Research Laboratories CIBA-Geigy Japan Ltd. (1990–93), and Vice-Head of Department of Molecular Behavioral Biology, Osaka Bioscience Institute (1993–98). From 1998, I have been the Head of forenamed and engaged in sleep research, Enzymology, Inflammation.

-1-

2.   I am one of the inventors for the invention described in U.S. Patent Application No. 10/520,781 and am familiar with the subject matter thereof.

3.   I have read the Office communication concerning the above-identified application issued on July 17, 2008.

4.   Under my direction, the following experiments have been done for the purpose of showing the effects of the antagonist against prostaglandin D receptors on the traumatic brain injury. They were evaluated by a mode of stab-wounded brain injury in mice (Salhia B, et al., Brain Res., 888:87-97, 2000; Asahi M., et al., J. Neurosci., 21:7724-7732, 2001; Garcia de Yebenes E., J. Neurochem., 73:812-820, 1999) as described in Examples 3, 6 and 7.

The effect of TM30089 (3-[(4-fluoro-benzenesulfonyl)-methyl-amino]-1,2,3,4-tetrahydro-carbazol-9-yl}-acetic acid) (Mathiesen JM, et al., Mol Pharmacol. 2006; 69(4):1441-53) or ONO-4127Na (-(p-butoxy)benzoyl-2-methylindole-4-acetic acid), (Qu WM et al., Proc Natl Acad Sci U S A. 2006;103 (47):17949-54)) which are known to be the antagonist of prostaglandin D receptors are on a model of stab-wounded brain injury was evaluated by a leakage amount of dye to the injured area (Kamimura et al.,Nature Medicine, 4:1078-1080, 1998).

Evans blue dye was intravenously injected on the second day after the brain injury and the amount of leaked dye into the tissue during 2 hours after the injection.

When TM30089 (30 mg/kg) or ONO4127Na (30 mg/kg) was orally administered 1 hour before and 1day after the occurrence of the injury, the increase in amount of leaked dye noted as a result of brain injury were suppressed (Fig).
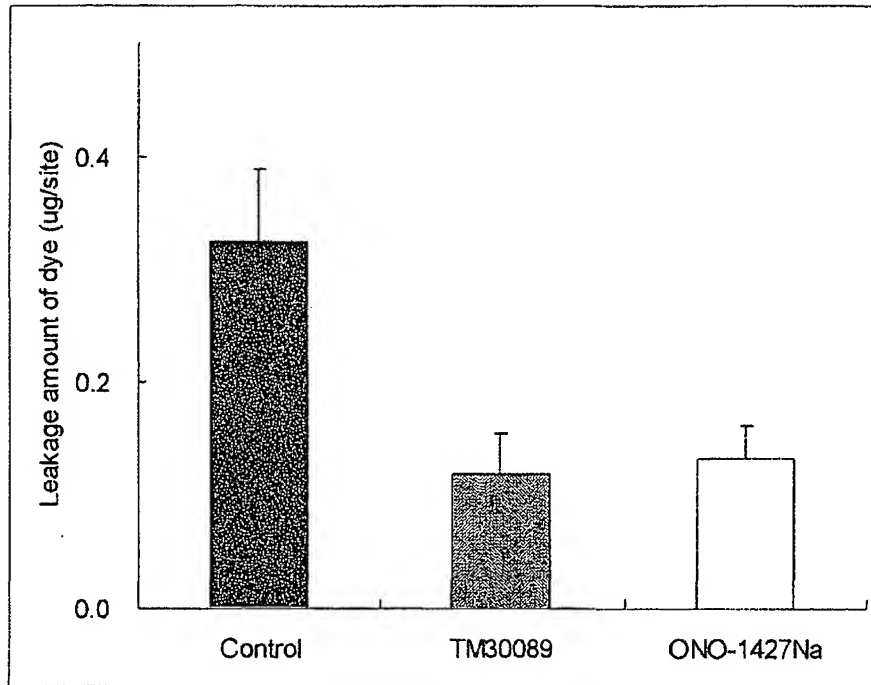
The undersigned declares further that all statements made herein of his own knowledge are true and that all statements made on information and belief are believed to be true; and further that these statements were made with the knowledge that willful false statements and the like so made are punishable by fine or imprisonment, or both, under Section 1001 of Title 18 of the United States Code and that such willful false statements may jeopardize the validity of the above-identified application or any patent issuing thereon.

This 9th day of December, 2008.

Yoshihiro URADE